SYNOPTIC CHARACTERISTICS OF INTENSE PRECIPITATION EVENTS IN THE SOUTHEASTERN UNITED STATES

by

WALKER JAMES SKEETER

JASON C. SENKBEIL, COMMITTEE CHAIR
DAVID J. KEELLINGS
GLENN A. TOOTLE

A THESIS

Submitted in partial fulfillment of the requirements
for the degree of Master of Science
in the Department of Geography
in the Graduate School of
The University of Alabama

TUSCALOOSA, ALABAMA

2018

ABSTRACT

The Southeastern United States is a region where increases in temperature have been largely muted when compared to other regions of the country, although extremes in both temperature and precipitation have become more common over time.

In the first part of this research, the strength and recurrence of Southeastern United States intense precipitation events (IPEs) was analyzed annually, seasonally, and sub-regionally with an emphasis on identifying trends and causal mechanisms at each of these temporal and spatial scales. Causal mechanisms responsible for IPE were investigated by utilizing the Spatial Synoptic Classification (SSC) to determine which surface weather types are associated with these events. Furthermore, a case study analysis of the most intense IPE in each physiographic province was performed with archived daily surface maps to classify the type of surface forcing mechanism that was responsible for the most exceptional IPE in each physiographic province. Results showed a statistically significant and regionally variable increase in both the recurrence and strength of IPE. A statistically significant increase in the number of moist tropical (MT) weather type IPEs per year was identified, and attributed to more common northward and inland encroachment of these events. Case study reveals that coastal areas depend heavily on tropical events and stationary fronts, while forcings in inland areas are more evenly distributed.

In addition to surface characteristics, the second part of this research explored synoptic patterns found with the most intense IPE across the entire study area. Principal Component Analysis, and Cluster Analysis were employed with 500 and 850 mb geopotential heights and a variety of seed variables in subsequent analyses to discover distinct types of IPE. A manual

classification based on IPE origin as either a warm or cold core system, and formation location of the IPE provided the best representation of the synoptic patterns responsible for types of IPE. These IPE types were portrayed via a series of mean flow maps of 500 and 850 mb geopotential height, sea level pressure, and 72 hour mean precipitation. The precipitation amounts of the 72 hour means for the five IPE types were statistically significantly different from each other.

LIST OF ABBREVIATIONS

IPE(s)	Intense Precipitation Event(s)
SSC	Spatial Synoptic Classification
MP	Moist Polar
MM	Moist Moderate
MT	Moist Tropical
TR	Transitional
IDW	Inverse Distance Weighting
SeUS	Southeastern United States
MLC	Mid-Latitude Cyclone
KW	Kruskal-Wallis

ACKNOWLEDGEMENTS

I would like to thank everyone in the University of Alabama Department of Geography, professors and fellow graduate students alike, who have helped along the way to completing this thesis, especially my advisor and committee chair Dr. Jason Senkbeil. His guidance throughout the last two years has been invaluable to my continued development as an academic, and I'm happy to call him a friend. I would also like extend a special thanks to Dr. David Keellings, and Dr. Glenn Tootle for taking the time to be members of my committee. Additional thanks goes to Dr. Keellings for writing the necessary code for this work. I know you said you enjoy doing it, but I'm sure it was a pain either way, so thank you.

I would like to thank all of the friends I have made during my time here at Alabama. I would list you all off, but I don't want anyone to think I'm playing favorites, so I'll just leave it at "you know who you are". My biggest worry about moving 1,000 miles away from home was that I'd have trouble making new friends. I'm happy to say two years later that I was able to, and hopefully the friendships I have made will last a lifetime. Roll Tide.

I would also like to extend my heartfelt thanks to the Salisbury University Department of Geography and Geosciences, specifically its former chair and my father, Dr. Brent Skeeter, and my undergraduate advisor Dr. Darren Parnell. Without the knowledge and experience I gained in my four years at SU before arriving in Tuscaloosa, the road to completing this research would have been much more difficult to traverse. Go Gulls.

Obvious thanks go to my mother. Thank you for keeping me in line, and making sure that I was ready when it was finally time to leave the Peninsula. Additional thanks to my brother,

Wesley, for always lending an ear when I hit snags in my work, and for all but introducing me to the subfield of hydroclimatology during that tram ride in Tampa. Catherine and Will, you both played huge roles in me becoming the person that I am today, mainly through your constant verbal jabs forcing me to develop a quick sarcastic wit. So I mean it when I say thank you.

CONTENTS

LIST OF TABLES

LIST OF FIGURES

CHAPTER 1

INTRODUCTION

While there is still considerable uncertainty as to whether overall precipitation totals will increase globally, regionally, annually, and seasonally in the future (IPCC Climate Change 2013: The Physical Science Basis Chapter 11), it is often anticipated that in a warming climate, intense precipitation events (IPE) will become more common as well as more extreme (Trenberth, et al. 2003; Emori & Brown, 2005; Janssen, Wuebbles, & Kunkel, 2014; Prein, et al. 2016). Despite this assertion, an implicit understanding of the surface and upper atmosphere synoptic patterns that create IPE is essential for accurate modeling and prediction (O'Gorman & Schneider, 2009; Nickl, et al. 2010; Sugiyama, Shiogama, & Emori, 2010; Pathirana, et al. 2014). This is especially true for the Southeastern United States (SeUS) which is subject to synoptic scale influences on IPE throughout the entire year (Schumacher & Johnson, 2006). Furthermore, the SeUS is a region that has been characterized by a muted or absent warming signal in temperature during 1951-75 (Rogers 2013; Pan et al. 2013; Meehl et al. 2015), but a warming signal is thought to have returned in more recent decades (Grose et al. 2017). Although this region has generally lagged behind model projections of temperature increase, relatively fewer studies have examined changes in precipitation events over time in the region. Thus, the importance of understanding the ingredients necessary for IPE, and historical precipitation and IPE trends is of great concern in the context of future model projections and climate change verification.

There is a large volume of literature surrounding observed and expected trends in IPE. IPE are expected to become more common over time, due principally to changes in atmospheric

motion, and atmospheric moisture that are expected to accompany a warming climate (Emori & Brown, 2005; Chou, et al. 2012; Fischer & Knutti 2016). It is predicted that overall precipitation intensity will increase by approximately seven percent worldwide, though this change is expected to be variable from region to region (Trenberth, et al. 2003) with a marked increase in heavy precipitation events, though this change is expected to be characterized by regional variability (IPCC Climate Change 2013: The Physical Science Basis Chapter 11). This anticipated regional variability is explored by Prein, et al. (2016) which postulates that hourly precipitation extremes in the contiguous United States will increase significantly in areas that have access to abundant moisture, but will decrease abruptly in moisture limited regions. In the United States, heavy precipitation events have shown evidence of increasing trends, particularly in the northeast U.S. (Collow et al. 2016), and also with mesoscale convective systems (Prein et al. 2017). The frequency and magnitude of the most extreme floods has increased dramatically in Europe and the United States for the period from 1980 -2009 (Berghuijs et al. 2017). Furthermore, Mallakpour and Villarini (2017) found evidence of increasing frequency of heavy precipitation events for most regions of the United States.

Modeling studies of precipitation intensity are not skilled at replicating inherent differences in precipitation at different latitudes (O'Gorman & Schneider, 2009). Models may be overestimating future changes in intensity, by exceeding the amount of atmospheric moisture that is available (Sugiyama, Shiogama, & Emori, 2010). A lack of homogeneity in experienced changes is true temporally as well, with Nickl et al. (2010) finding that the first half of the 20th century (1902-1949) saw an increase in annual precipitation while the period from 1949-1993 saw an overall decrease in annual precipitation. That trend again reversed itself, with the period of 1992-2002 showing an increase of approximately 0.75-2.1 mm/yr. Alexander et al. (2006)

found a significant increase in global precipitation by piecing together a network of standardized analyses to create a comprehensive global picture of extreme precipitation indices. Extreme precipitation indices, and subsequently the frequency of intense events, are expected to continue increasing throughout the next century (Janssen, Wuebbles, & Kunkel, 2014).

A study of northeastern US precipitation conducted by Agel et al. (2015) examined the top 1% of wet days across a network of surface stations, and found that in the northeast, 90% of intense events occur at only 1-3 stations concurrently. The study also found that in an individual intense event, 50% of the total precipitation for that event typically falls within the span of three hours or less. The role of teleconnections and large scale atmospheric circulation has also been explored as a way of explaining observed changes in precipitation trends and regimes. Changing phases of teleconnections lead to large scale variability in precipitation totals on annual to decadal time scales, which complicates the process of analyzing and making assertions about underlying causes of climate system responses. (Hurrell 1995; Keim 1997; Trenberth et al. 2003; Krichak et al. 2012). Land use changes that coincide with population growth are also a factor in precipitation trends, as it has been shown that increased urban land use will lead to higher precipitation values downwind of the developed areas than would be expected if the areas were under a natural land use regime (Pathirana, et al. 2014).

Specific to the Southeastern US (SeUS), Keim (1996) synoptically classified IPE (defined as any two-day period of three or more inches of liquid equivalent precipitation) for eight weather stations across the SeUS as either frontal, tropical, or airmass events, and found that frontal events were the dominant forcing mechanism in the SeUS. Keim (1997) used similar methodology, utilizing 27 observation stations with an average across those stations of 92 years' worth of records, and found that in the SeUS, the Gulf Coast received the most intense events,

while the Appalachians and Texas received the fewest. The study also found that the Southeast Coast exhibited a small decline in the total number of intense events per year. This Southeast Coast decline was confirmed by Frich (2002), and again by Powell & Keim (2012), who additionally found that both precipitation and temperature extremes are becoming more common over time. The eastern portion of their study area, particularly South Carolina, was again found to defy the increasing IPE trend that the rest of the region is experiencing. Kunkel (2012) examined all "one in five years" strength events across the US, and determined that for the Southeast, tropical systems were responsible for 51% of these anomalous events, while frontal events were responsible for 34% of such events. Outside of the Southeast, the study showed that for the contiguous US, frontal events accounted for the majority of intense events, at 54%, showing a notable difference between the Southeast's synoptic mechanisms when compared to the rest of the country.

Moore et al. (2015) conducted a radar based study, which utilized 24-hour multi-sensor precipitation analyses as a means of avoiding the spatial variability that is introduced by using ground based observation stations, to synoptically analyze all 99^{th} and 99.9^{th} percentile precipitation events in the Southeast. It was found that non-tropical IPE form in both strongly synoptically forced scenarios, and weakly forced scenarios. The precipitation totals of IPE that form under a weak synoptic regime are more difficult to forecast. Schumacher & Johnson (2006) explored the seasonality of intense events in the SeUS, finding that while the northern US experiences intense precipitation events almost exclusively during the warm season, the SeUS experiences IPE throughout the entire year due to relatively warm winter temperatures and access to warm water.

There is also a large volume of literature that explores potential environmental, hydrological, and other hazardous impacts of changes in precipitation trends and extremes, which highlights the importance of understanding these changes. The global hydrologic cycle is expected to enhance as climate warms, which will lead both to larger events, and longer periods of time between events. This change in precipitation will alter soil moisture and the health of plants significantly (Weltzin et al. 2003; Seneviratne et al. 2010; Zeppel, Wilks, & Lewis, 2014). It is important to note however that intense precipitation events impact different landscapes in different ways. For instance, more intense but less frequent rainfall events will likely lead to increases in primary production in xeric (low moisture) environments such as semi-arid grasslands (Heisler-White et al 2008), as well as increases in primary production in hydric (high moisture) environments, however this same type of change in precipitation regime will likely decrease primary production in mesic (moderate moisture) environments, principally by increasing runoff and deep drainage (Knapp et al 2008). The presence of a more episodic precipitation regime also has the potential to increase the chance for drought, which has the potential to lead to mass die-offs of forests and other vegetation, which can alter surface-atmosphere interactions (Anderegg et al. 2013). Additionally, it cannot be ignored that increases in the occurrence of IPE is likely to lead to an increase in flood and landslide events which have the potential to adversely impact human infrastructure and life (McGuire, 2010). In the United States, heavy precipitation events and flooding have caused considerable property damage despite federal and local policy initiatives to mitigate impacts over time (Brody et al. 2011). The frequency and magnitude of the most extreme floods has increased dramatically in Europe and the United States for the period from 1980 -2009 (Berghuijs et al. 2017). It is important to realize however that intense rainfall is not the only reason that flooding occurs, as rain induced

hydrologic flooding is also driven by soil moisture, topography, and other variables (Kunkel, 1998). Further, the danger to human life posed by IPE is not limited to floods and landslides, with Curriero et al. (2001) finding that 51% of reported waterborne disease outbreaks were preceded by a precipitation event above the 90^{th} intensity percentile, and 68% of outbreaks were preceded by an 80^{th} percentile event.

In this research, IPE trends were evaluated both spatially and temporally for 56 stations across a ten state region encircling the SeUS. The main questions that will be explored within this research are as follows:

1. Are IPE becoming more common over time?
2. Are IPE becoming more intense over time?
3. What is the seasonality of IPE?
4. What Spatial Synoptic Classification (SSC) categories are the most common with IPE?
5. Is the SSC an effective tool to classify IPE?
6. Are there commonly recurring upper atmospheric patterns associated with large scale IPE?

CHAPTER 2

JUSTIFICATION

While an expected increase in IPE intensity and recurrence is a fairly well accepted phenomenon within the climatological community, this research seeks to explore the issue in a variety of unique ways. Firstly, this research utilizes the Spatial Synoptic Classification (SSC) (Sheridan 2002) by assigning every IPE an SSC classification. Based strictly on surface observations at individual stations in the US and Canada, the SSC is a weather type classification scheme. Given that it does not take upper atmosphere conditions into consideration, it is not an airmass classification scheme like the Bergeron classification scheme. The SSC has seven weather type classes, though given the nature of the SSC and precipitation events, none of the three dry weather types are used. The remaining weather types are:

+ **Moist polar (MP) -** Subset of mP Bergeron class. Cloudy, humid, and cool conditions. Primarily created through inland transport of cool maritime air.

+ **Moist moderate (MM) -** Markedly warmer and more humid than MP. Often occurs in synch with MP, but further south.

+ **Moist tropical (MT) -** Synonymous with mT Bergeron class. Associated with warm sectors of cyclones, or the western side of an anticyclone. Due to MT's dominance in tropical regions, MT+ and MT++ were developed to represent excessively humid environments.

+ **Transitional (TR) -** Days in which one weather type yields to another.

*All SSC descriptions acquired from http://sheridan.geog.kent.edu/ssc.html (Sheridan, Spatial Synoptic Classification, n.d.)

Archived daily maps of SSC classifications across the US and Canada are available online for the period from 1948-2016, and are updated annually to include the previous year's data (Sheridan, Spatial Synoptic Classification, n.d.). Using the SSC scheme to classify IPE is effective in that the SSC takes multiple variables about a given location's current surface conditions, and synthesizes them into one representative variable, which facilitates efficiency. Manually classifying each IPE based on surface forcing mechanisms was also considered, but deemed too laborious with more than 7,500 individual events, and deemed too subjective.

This research also assesses the utility of using SSC classifications to identify distinct synoptic IPE regionality. Identifying regionality based on SSC recurrence has not been attempted before. As such, this research has the potential to open new avenues for future research involving the SSC as it relates to precipitation, drought, and other rainfall related phenomena. Previous research conducted by the author on smaller scales (1-4 states) has successfully identified distinct synoptic regionality of surface forcing mechanisms using an isocluster analysis in GIS of IDW surfaces based on the recurrence of IPE caused by those various surface forcings. This research attempts to identify synoptic regionality of IPE in a similar way, but uses the seasonal distribution of SSC classifications at each location rather than surface forcing mechanisms. Being able to identify synoptic regionality is useful in that it provides a statistically derived way of identifying regions based on precipitation regimes. This allowed a study area to be divided into a variety of regions for the purpose of statistically analyzing synoptic scale trends between them. In the context of this research, identified regions are used to analyze seasonality and changing annual trends of IPE, as well as classify the surface forcing mechanisms associated with each regions most intense IPE.

The primary implications of this research lie in agricultural and local water budget applications. It is important to know whether IPEs are becoming more common or stronger over time, and where these changes are greatest. If the hypothesis of more frequent and stronger IPE over time is true, then that information can allow for necessary changes to be made to current water resource management policies, especially in areas that are more dependent upon episodic intense events to recharge their water supply. Furthermore, it is important to identify how these trends vary across the different regions throughout the study area, so that localities that are not heavily impacted are not making unnecessary changes. Additionally, this research has the potential to provide useful information to forecasters attempting to predict rainfall totals associated with exceptional events. This research can help forecasters make more informed predictions of the rainfall totals associated with events that take place under certain synoptic regimes, both at the surface and upper atmospheric levels.

CHAPTER 3

SURFACE LEVEL ANALYSIS: METHODOLOGY

Daily precipitation totals from 1950-2016 were collected from the National Climate Data Center (NCDC) for 56 surface observation stations across the SeUS. The definition of SeUS that is used in this research is all areas south of the Mason-Dixon Line (northern border of Maryland; 39°43′ N), and east of the Mississippi River. Each observation station had at least 95% data coverage, and of these stations, 41 were first order stations. The remaining stations used were second order stations located at regional airports (4), research centers/universities (2), or independently operated locations (9). The study area can be seen in figure 1.

Once all daily data was collected and organized by state, a script was written in R to identify all distinct precipitation events. For the sake of this research, a precipitation event is defined as any set of consecutive days with measurable precipitation. See below for an example:

10/16/1994	0
10/17/1994	0.15
10/18/1994	0
10/19/1994	1.5
10/20/1994	0.08
10/21/1994	0

← Event 1: 0.15 in.

← Event 2: 1.58 in.

It is noted that this definition could potentially lead to anomalously high rainfall totals for individual events, or that two synoptically distinct events may be inadvertently lumped together into one event. However, it was determined that the utility of identifying continuous periods of precipitation outweighed these risks, due to the fact that long periods of time with continuous or

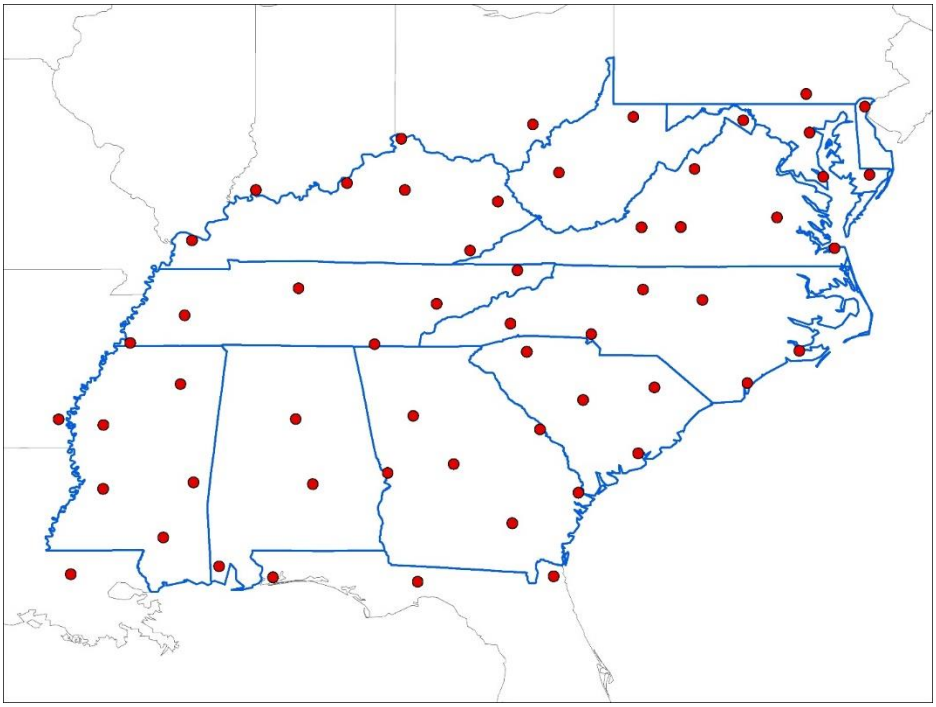

Figure 1: Study area with 56 observation stations used in this research.

near continuous periods of precipitation do not allow for soil moisture to adequately evaporate, which can lead to hydrologic flooding events.

Recognizing this potential issue, steps were taken to avoid over-representing long term, but not otherwise intense events, while ensuring equal representation of short term but otherwise intense events. Precipitation amounts from both could possibly be the same, but the shorter more intense event produces more runoff and has greater flood potential. A simple normalization equation was created to partition fair representation of both short term and long-term events:

$$\left(\frac{Event\ Total\ Precipitaion}{Event\ Length}\right) + Most\ Intense\ Daily\ Precip\ Total$$

Taking the average of the total precipitation produced by a given event reduces the resultant "normalized strength" associated with exceedingly long-term events, while adding the highest

daily total to the average allows any long-term events that were associated with an embedded intense single day total to still be represented.

Once each distinct event was identified and normalized, every event at each of the 56 locations was assigned a z-score, based on the normalized event strength. After z-scores were assigned, each location's 99th percentile events were identified and extracted. These 99th percentile events are defined as intense precipitation events (IPE), and were used as the basis for all statistical analysis. This method was deemed most appropriate due to the fact that using 99th percentile events relative to each location creates a similar sample size of IPE at each location. A static absolute threshold method similar to that utilized by Keim (1996) was considered, but previous research conducted by this author involving observation stations in mountainous and coastal regions of Virginia and Maryland showed this methodology leads to skewed sample sizes between coastal and inland areas, with coastal areas having significantly more events.

Once all IPE were identified, each event was assigned an SSC classification. As was explained on page 6, the SSC is a daily surface weather type classification that assigns a given location's daily surface weather conditions into one of seven potential classifications. When assigning SSC classifications to individual IPE that spanned multiple days, the day within the IPE that experienced the most precipitation was used as the day to assign that event's SSC classification from the SSC archive. This technique was used because the day within an event with the most precipitation is inherently the most "intense", and the basis of this research as it relates to the SSC is largely to "test the utility" of the scheme to classify intense precipitation events. It is understood that this methodology has the potential to introduce bias in IPE that experience a relatively uniform distribution of precipitation per day. Fortunately, this is not a particularly common occurrence. Based on a sample of 6 randomly selected stations used in this

research, only 6.6% of IPE experienced precipitation totals between the most and second most intense days in the event within 1 inch of each other. That percentage drops to 2.7% when the threshold is lowered to .5 inches. Generally, IPE have a clearly defined most intense day.

This research also seeks to evaluate the utility of using the SSC to identify synoptic and seasonal regionality of IPE. This is attempted through an isocluster analysis in GIS, which has effectively been used in previous precipitation based climate research (Yang et al. 2015). An IDW interpolated surface was created for the seasonal distributions of all four utilized SSC classifications, and an additional IDW was created of the average strength of IPE across the study area. In total, 17 IDW maps were created, and imported into an isocluster analysis, which were used in an attempt to identify regions within the study area where multiple stations have similar SSC distributions. Previous research by this author has shown that it is possible to use an isocluster analysis to identify distinct synoptic regionality based on the surface forcings that cause IPE. With over 7,500 total IPE across all stations in this research, a more efficient alternative was sought, as surface forcings would have to be manually classified based on archived surface maps. If it is found that the SSC is able to produce meaningful regionality, it can be confirmed as a useful alternative to surface forcings. Two different techniques were also used to manually split the study area into implicitly meaningful, though not statistically defined regions. Firstly, the study area was split into the dominant physiographic provinces that are within it, and secondly the study area was separated into 5 regions based strictly on latitude.

Identified regions were then utilized for more specific temporal analysis, to reveal which regions within the study area have experienced larger or smaller changes in the recurrence and intensity of IPE. Physiographic regions were also used to assign surface forcing mechanisms to each region's top 30 most intense IPEs, to identify the surface forcings that are responsible for

the most intense IPEs across different parts of the study area. A threshold of 30 IPE was used in order to be able to assert statistical relevance, while not expending excessive time on manual analysis. Further, to avoid over representing an individual observation station within each region's top 30 IPEs, if a given station had more than 5 events within a region's top 30, only that station's 5 strongest IPEs were used, and the next strongest IPE at other stations were instead utilized. A scheme similar to that utilized by Keim (1996) was utilized to classify each of these events into one of the following classes based on archived surface maps: airmass, frontal (warm, cold, or stationary), low pressure (concentric, or with frontal influence), tropical (both tropical, and extratropical), or a combination of these. This allows for additional synoptic differences between the regions to be identified and analyzed.

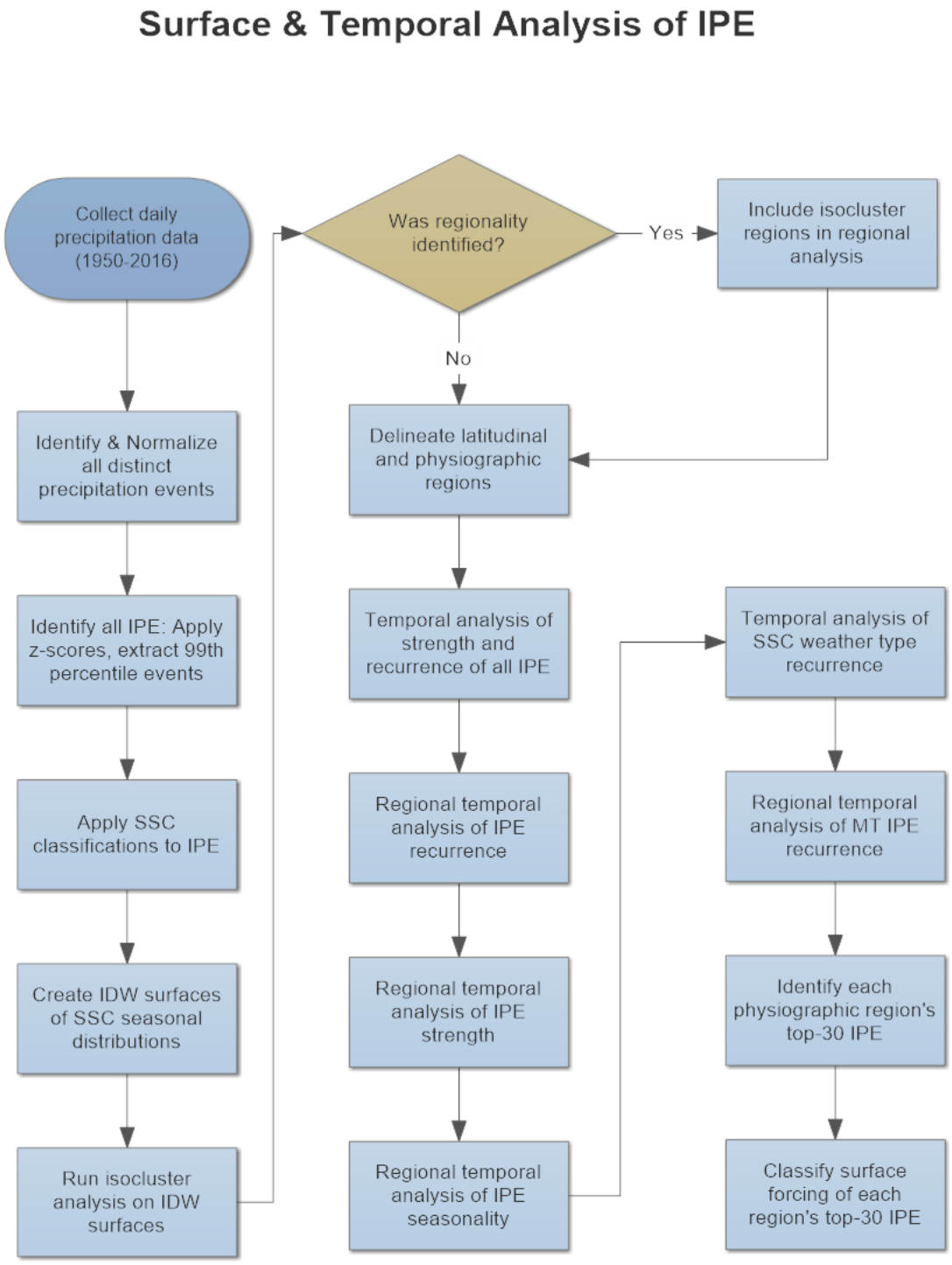

Figure 2: Flowchart showing steps discussed in Chapters 3 and 4.

CHAPTER 4

SURFACE LEVEL ANALYSIS: RESULTS & DISCUSSION

The total number of IPE identified across the study are was 7,704. Each of these events was assigned an SSC surface weather type classification. Of these 7,704 IPE, 24 were not assigned an SSC classification due to issues with the map archive not displaying data for the day in question, resulting in a total of 7,680 total IPE that received an SSC classification. The distribution of SSC classifications across the study area can be seen in figure 3. The dominance of the moist moderate (MM) classification was an unexpected result, as it was anticipated, especially in the Southeast, that the moist tropical (MT) classification would be dominant. On the contrary, both MM and transitional (TR) weather types occur more frequently than MT weather types. The seasonal distributions of each SSC class were graphically analyzed as well, and can be seen in figure 4.

A potential cause for the unexpected dominance of the MM weather type is that when a rain event occurs, it has a dampening effect on air temperature due to cloud cover at that location. Bearing in mind that the SSC is a surface weather type classification scheme, surface temperature is one of the primary inputs when an SSC classification is assigned. As such, when an intense or prolonged precipitation event occurs, surface temperatures are often times lowered by the event and a more moderate SSC classification is assigned, even if the airmass is tropical in nature or origin.

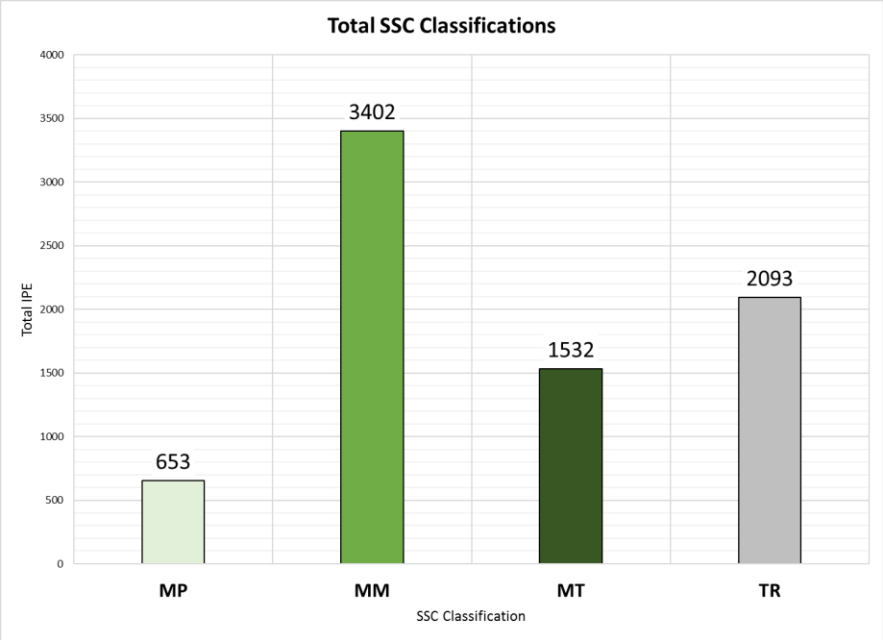

Figure 3: SSC weather type distribution of all IPEs

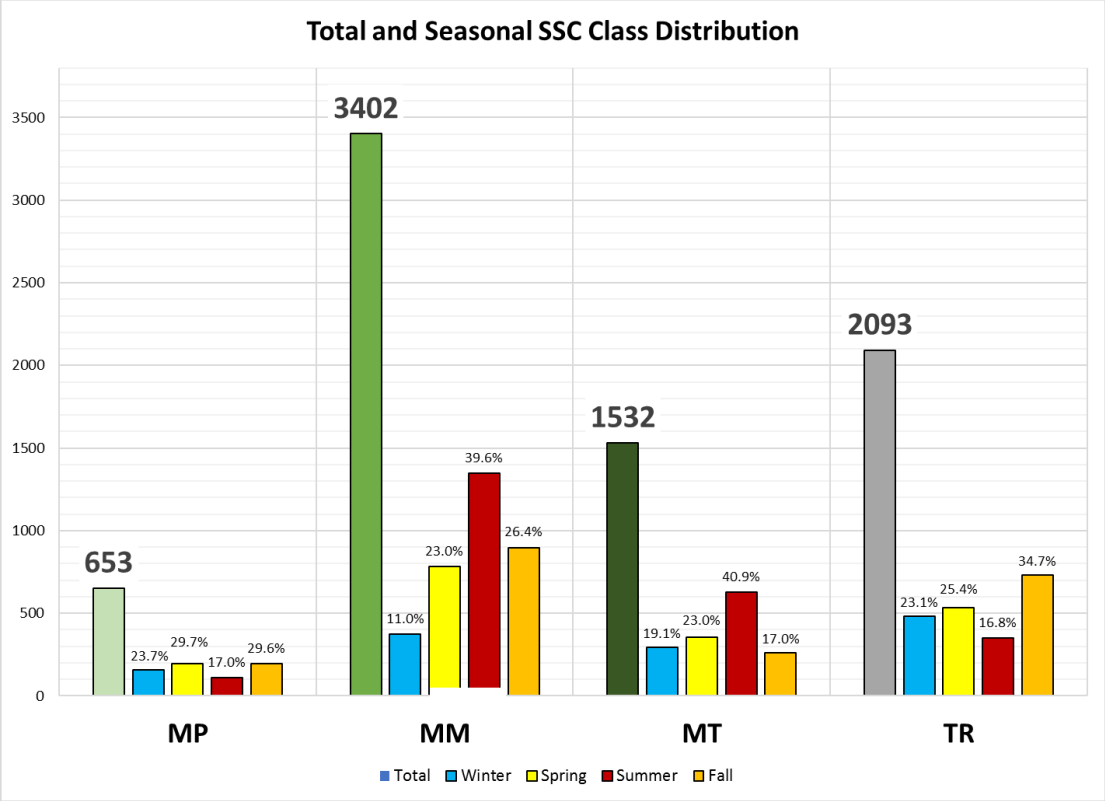

Figure 4: Seasonal distribution of SSC weather type classifications. Percentage values indicate the percentage contribution of each season to the respective SSC classification's annual total.

The seasonal distribution of each SSC classification was used as the basis to attempt to create a synoptic regionality isocluster map. As was explained on page 13, an IDW interpolated surface was created for the seasonal distributions of all four utilized SSC classifications, and an additional IDW was created of the average strength of IPE across the study area. In total, 17 IDW maps were created, and were imported into an unsupervised isocluster analysis in GIS, which attempted to identify regions within the study area where multiple stations have similar SSC and IPE distributions. Through upwards of 60 different iterations, utilizing different numerical inputs, and different cluster sizes, it was deemed that the isocluster analysis was not able to produce meaningful synoptic regions. The best output, which utilized default input values, can be found in figure 5.

Those results, while not entirely useless, are not particularly helpful for statistical analysis of this nature. While the locations within each identified region do have similar SSC distributions, it would be inappropriate to imply that, for example, Savannah, GA and Paducah, KY, two locations separated by a mountain range and more than 500 miles, are synoptically similar. As a result, it is clear that on this large of a scale, using the SSC to identify synoptic regions based on IPE is not a viable methodology, and the regions that were identified have not been used in any forthcoming analysis. As was previously stated however, these results are not useless as the isocluster did show a fair amount of skill in separating the northern Appalachians, and two distinct regions in the deep south. Future research should be conducted to identify more effective ways to utilize isocluster analysis for identifying synoptic regions, possibly using surface forcing mechanisms as the criteria instead of the SSC, or as an additional input alongside the SSC.

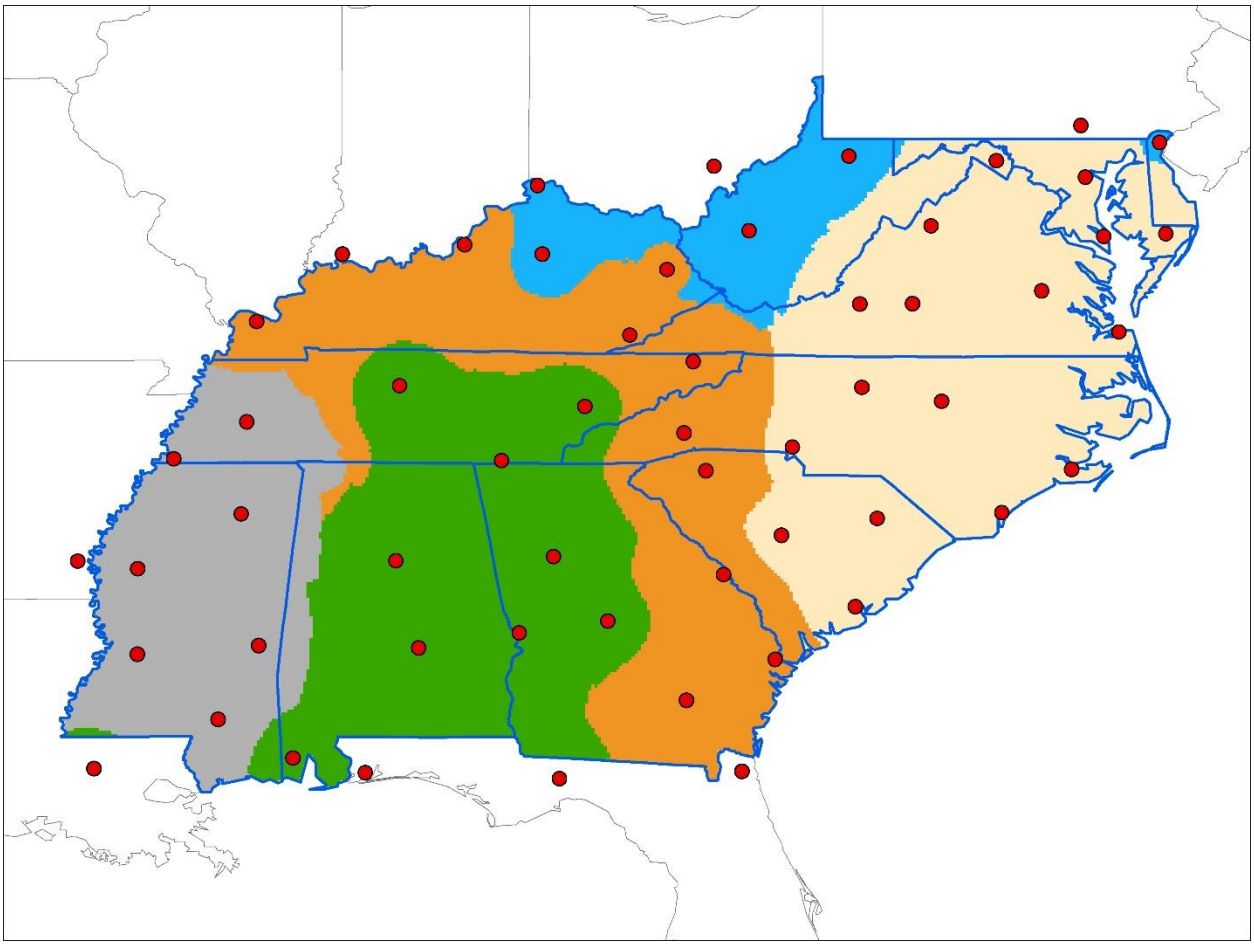

Figure 5: Attempted Isocluster results, utilizing default numerical inputs

As was described on page 14, manually defined regions based on (1) latitude, and (2) physiographic provinces were created. Latitude and physiographic provinces have been utilized for statistical analysis in previous climate research, with Senkbeil et Al. (2017) utilizing latitudinal regions to examine SSC weather type spatial distributions, while Barros et al. (2017) studied decadal scale influences on hydrologic drought within physiographic provinces of the SeUS. For the latitudinal methodology, 5 simple north-south regions were identified with equal sample sizes, while physiographic regions were based on a USGS map downloaded via ArcGIS Online (Fenneman & Johnson, 1946) (Figure 6). The original iteration of this map had 6 major, and 17 minor physiographic provinces within the study area. In order to allow a meaningful

sample size within each region, coastal and highland provinces (both major and minor) were consolidated together and slightly altered to create the physiographic map in figure 6. This produced 5 dominant physiographic provinces. These provinces (as well as the total number of stations within them) are both the Atlantic (15) and Gulf (13) Coastal Plains, the Piedmont (7), the Appalachian Highlands (13), and the Ohio-Mississippi Valley (8). In order to create equal sample sizes, The Ohio-Mississippi Valley sub-region was constructed by combining five stations of the Interior Low Plateau region with three stations on the northern reaches of the Gulf Coastal Plain (see Figure 1). The three northern Gulf Coastal Plain stations that were added to the Ohio-Mississippi Valley sub-region had more in common climatologically with the five Interior Low Plateau region's stations due to their inland location away from mesoscale convective warm season processes, such as the sea breeze. Both the latitudinal and physiographic regions were utilized for performing spatially derived statistical and temporal analysis of all major variables.

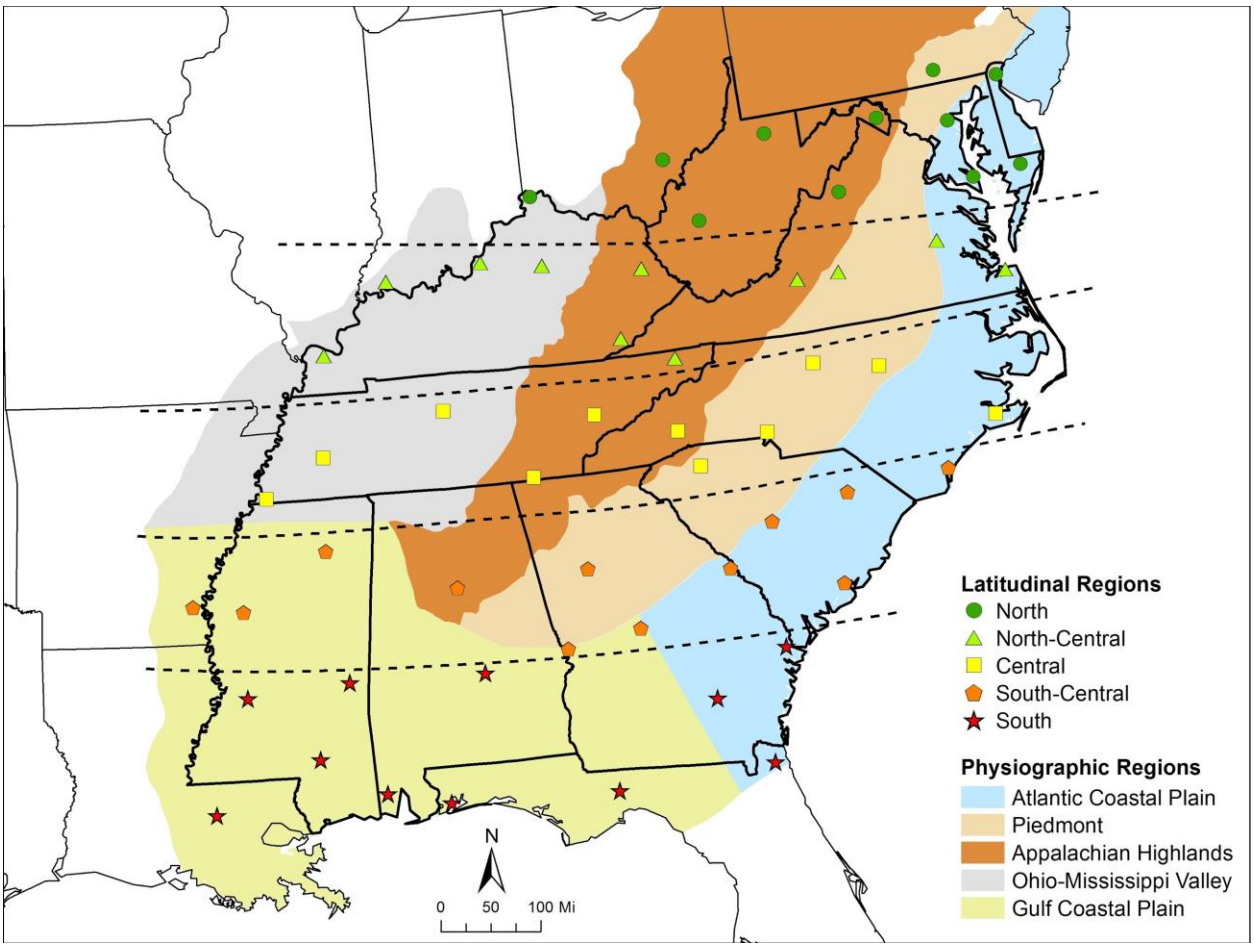

Figure 6: Physiographic (color coded) and latitudinal (dashed lines & shape coded) regions.

Ordinary least squares (OLS) regression was used to test for annual, and seasonal trend significance. Non-parametric Mann-Kendall slope tests were used in conjunction with OLS regression for locations with non-normally distributed data. IPE trends at each location were tested for normality using a Shapiro-Wilk test. IPE recurrence and intensity trends were analyzed across the entire study area, and regionally (physiographic and latitudinal divisions) to identify regions across the study area where increasing or decreasing trends are more enhanced. Results of the following sections can be viewed in table format in table 1 on page 36.

Annual recurrence of IPE: Across the entire study area, IPE show a statistically significant increasing trend ($p = 0.013$) in annual recurrence (figure 7). Since 1950, the annual number of IPEs is increasing at a linear rate of 0.38 events per year. This corroborates the findings of Mallakpour and Villarini (2017) whom, using a 95th percentile peaks over threshold method, found that 19.3 percent of the pixel area of the region has experienced significant increases in extreme precipitation events. As can be seen in figure 7, from 1950-1963 there was not a noticeable increasing trend, and there was relatively little variability from year to year. The period from 1963-2016 however is marked by large annual variability in the total number of IPE, as well as an increasing trend that is marked by higher peaks, and less extreme valleys. As was discussed by Krichak (2012), the phases of certain teleconnections play a significant role in annual variability of IPE recurrence. While teleconnection phases are the most likely explanation for observed annual variability, they do not effectively explain the statistically significant increase in total annual IPE. Emori & Brown (2005) assert that increases in atmospheric motion and moisture are expected to lead to increased recurrence of IPE. That is believed to be the primary underlying cause of the increasing trend observed here.

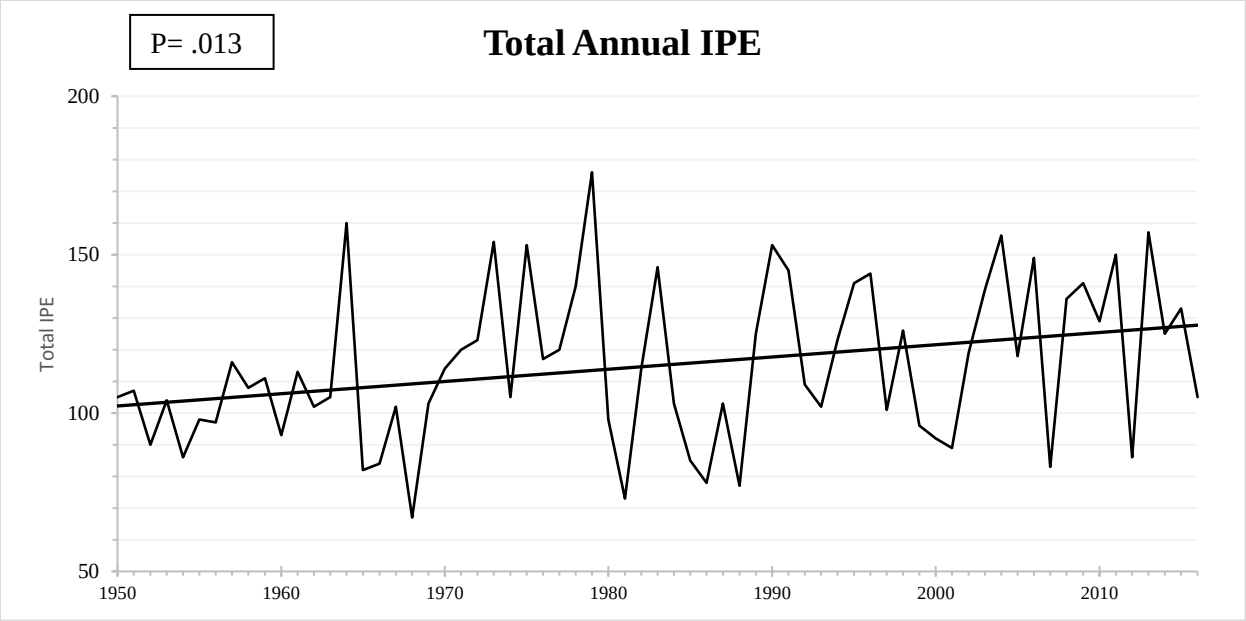

Figure 7: Total number of IPE per year across the entire study area. Significance value (P-Value) obtained via a linear regression test.

Average strength of IPE: Along with the total number of IPE increasing per year, it is also anticipated that the average strength of IPE has increased over time. As can be seen in figure (8) this speculation has been confirmed through the identification of a statistically significant increase in the average normalized strength of IPE since 1950 ($p = .005$).

It is important to note that the 'normalized strength' of the events is the metric that is used in the following analysis, rather than the total amount of precipitation associated with an event. There is high confidence in the effectiveness of the normalization, as well as its ability to effectively portray the increasing strength of IPE over time. Even though normalized strength is used as the represented variable, it has been confirmed that an increase in the average normalized strength of IPE is reflected by an increase in the total amount of precipitation associated with IPE since 1950 ($p = .008$), which can be seen in figure (9). Both the frequency and intensity of IPEs

are significantly increasing in the region suggesting that the forcing mechanisms responsible for IPEs are becoming more common, more volatile, or perhaps characterized by greater longevity.

With statistically significant increasing trends in both the annual total and average intensity of IPEs identified, it is important to identify what regions within the study area are contributing the most to the significance of these trends. The following sections utilize the previously discussed regional delineations to identify areas of both enhanced and less severe increases in the annual number and intensity of IPEs. Results of all regional analyses are discussed individually, starting with analysis of the total number of IPEs per year, then the average normalized strength of each region's events.

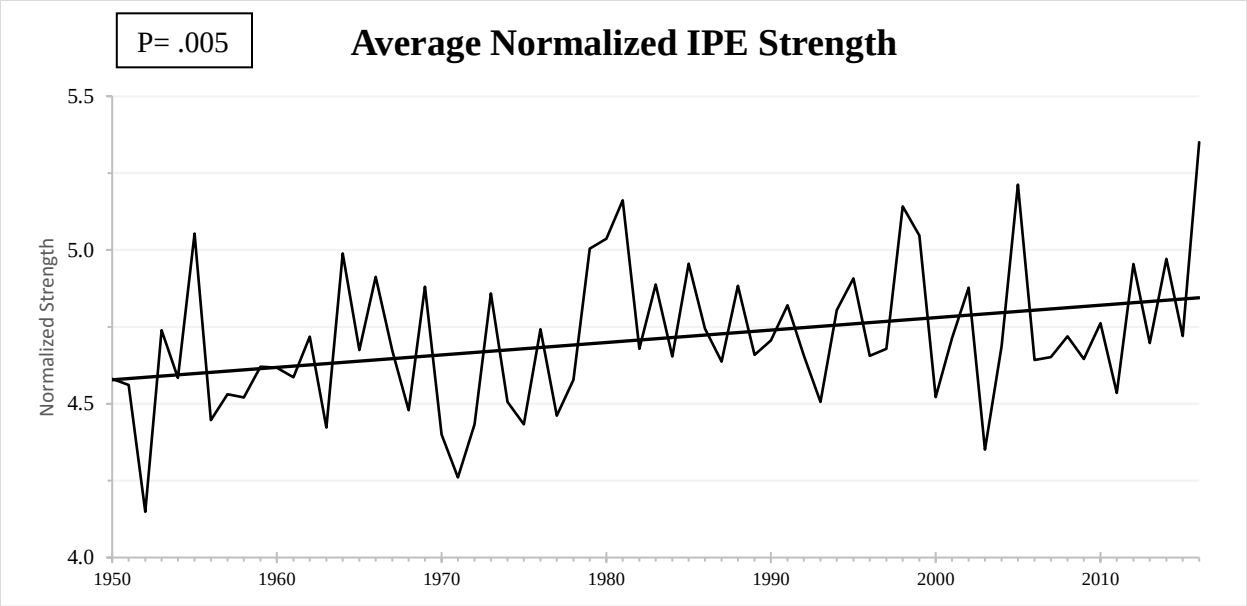

Figure 8: Average normalized strength of all IPE per year across the entire study region. Significance value (P-Value) obtained via a linear regression test.

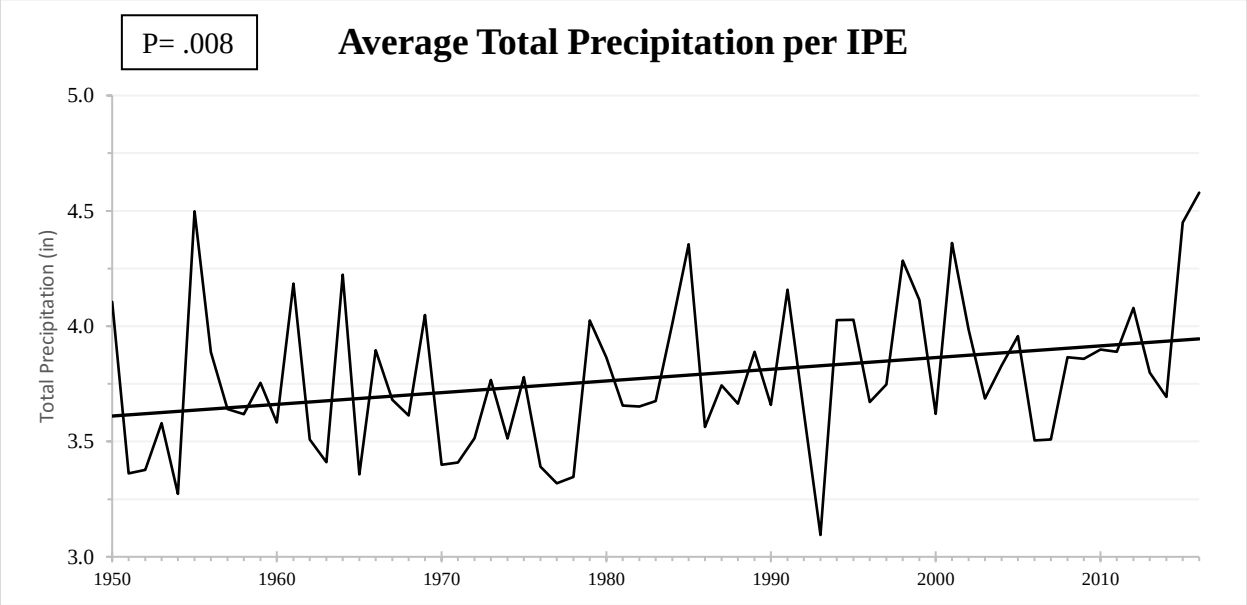

Figure 9: Average total amount of precipitation associated with each IPE per year across the entire study area.

a. Regional IPE Recurrence

Latitudinal (Total IPE): All latitudinally derived regions in the SeUS have experienced at least a slight increase in the total number of IPE per year on average. This increase is statistically significant at a 95% CI for both the North ($p = .049$), and the North-Central ($p = .031$) regions, but was not significant in the three southern regions (Figure 10). These results are meaningful, in that they indicate that as one progresses further northward, a more marked increase in the total number of annual IPE can be expected, meaning that while the entire study area has experienced a general increase, the most significant changes have occurred in the Northern regions. An explanation for increasing IPE with latitude is possibly due to changes in surface weather type frequency, markedly more common northward and inland incursion of warmer, tropical origin weather types, which is discussed in later sections. No individual region appears to be experiencing markedly more variability than the others, indicating that the total number of annual IPEs is consistently variable across all latitudes in the SeUS.

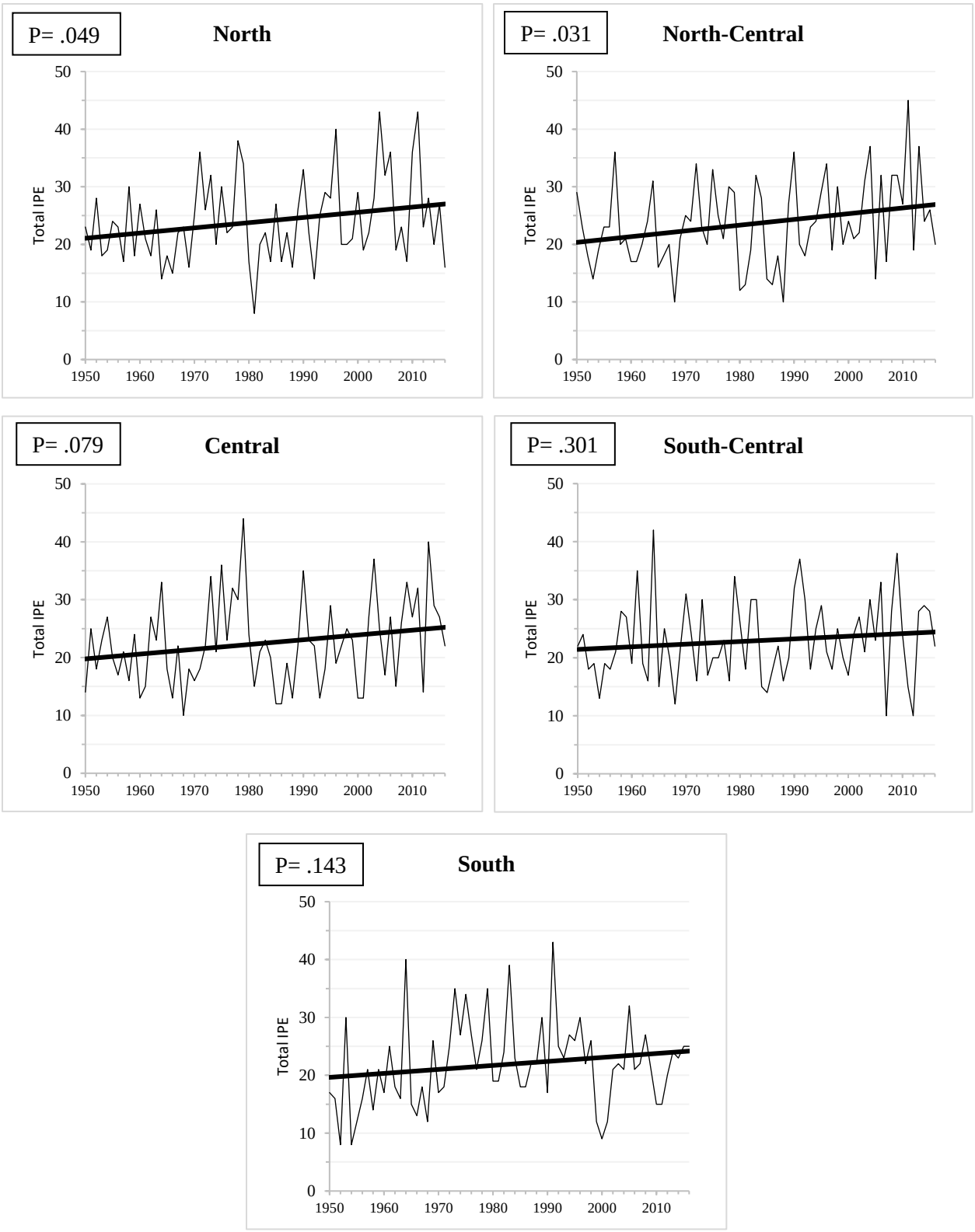

Figure 10: Total number of IPE per year in each latitudinal region

Physiographic (Total IPE): Similar to the latitudinal results, all physiographic provinces, except for the Atlantic Coastal Plain, are experiencing slight increases in the total number of IPE per year. The Atlantic Coastal Plain ($p = .757$) is experiencing only a minute increase, as well as extreme annual variability. This variability can likely be attributed to its proximity to the Atlantic Ocean and influences from large scale teleconnections (Tootle et al. 2005, Mallakpour and Villarini 2017) that influence synoptic scale trends, and can alter the path of storms closer to or farther from the coastline. At a 95% CI, the Ohio-Mississippi Valley ($p = .011$), and Gulf Coastal Plain ($p = .028$) regions are both experiencing statistically significant increases in the total number of IPE per year. This result appears to indicate that areas to the West, and to the South of the Appalachians have experienced a more significant increase in the total number of IPE than areas within or to the East of the Appalachian Mountains. The Appalachian Highlands ($p = .066$) has also experienced large annual variability similar to that of the Atlantic Coastal Plain, while the Piedmont ($p = .08$) is experiencing markedly less annual variability than the other regions, which can be attributed to a lower number of stations within the region.

The physiographic results appear to somewhat juxtapose the latitudinal regionality results, as latitudinally the southernmost regions are not experiencing statistically significant change, but physiographically the second most significant change is along the Gulf Coastal Plain. This discrepancy is driven principally by the South region including multiple locations in the Atlantic Coastal Plain, which has not experienced a significant increase, and the inclusion of points located further north in Mississippi in the Gulf Coastal Plain region that are not in the South region.

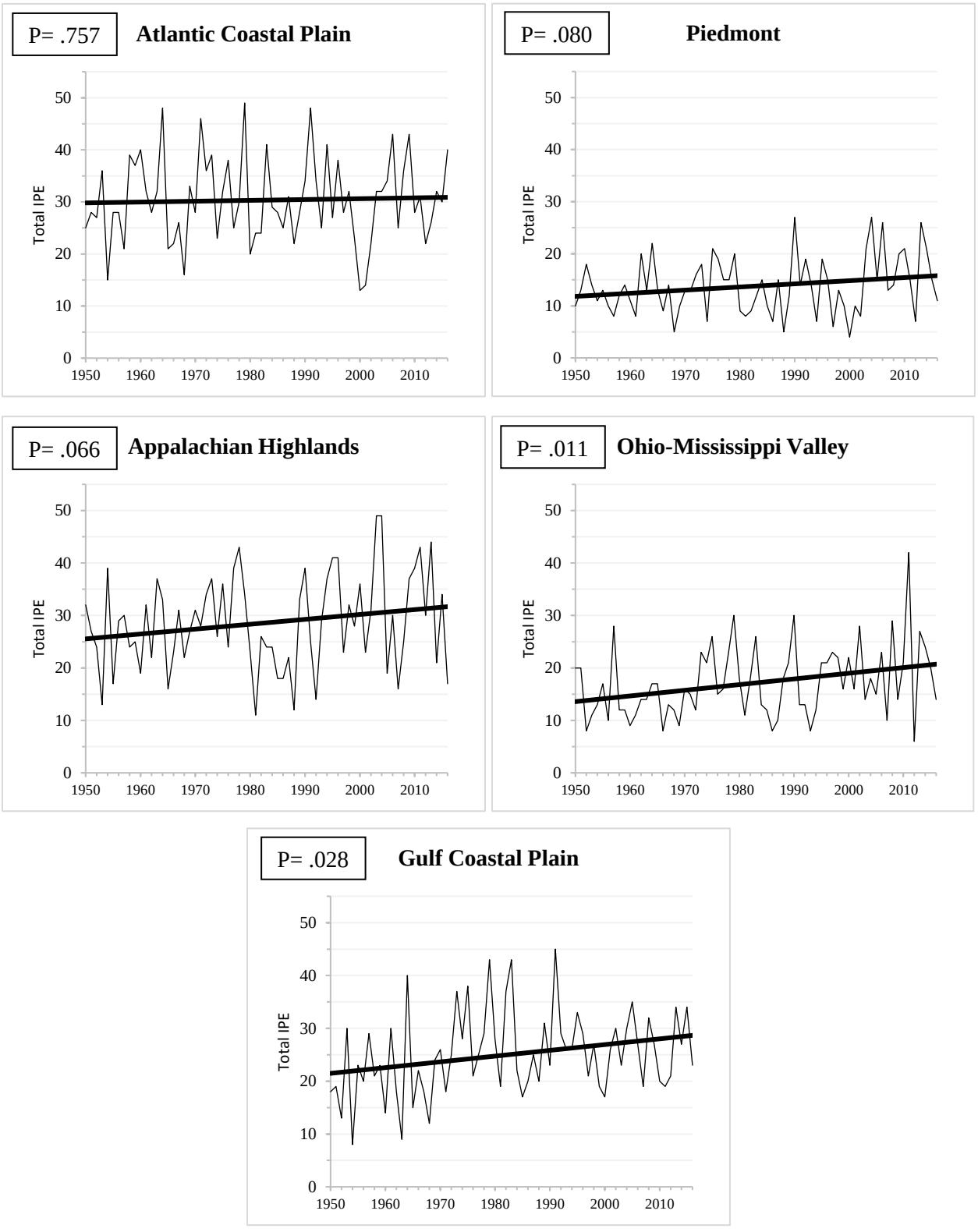

Figure 11: Total number of IPE per year in each physiographic region

b. Regional IPE Intensity

Latitudinal (Normalized Strength): All regions within the study area have experienced a slight increase in the average normalized strength of IPE per year, however according to OLS regression, none of these regions are experiencing a statistically significant increase at a 95% CI. Although the study area as a whole is experiencing a significant increase, it appears that when the study area is partitioned latitudinally there is simply too much annual variability in each region, especially the south region which despite drastic annual variability has experienced the most noticeable increase in IPE intensity, to assert with high confidence that any individual latitudinal ranges are experiencing a more marked increase in IPE strength than the others. The two southern regions have the highest average strength of IPEs, which is not surprising given the frequency and strength of tropical origin events and ample year-round moisture supply in these areas. These two regions have also experienced noticeable, though not statistically significant increases in event strength. Considering this, while it cannot be stated with very high confidence that any latitudinal ranges are experiencing significant changes in IPE strength, it can confidently be stated that the southern regions of the study area have contributed more to the study-area wide increase in average IPE strength than the northern regions, and that their IPEs are generally more intense than the more northern regions.

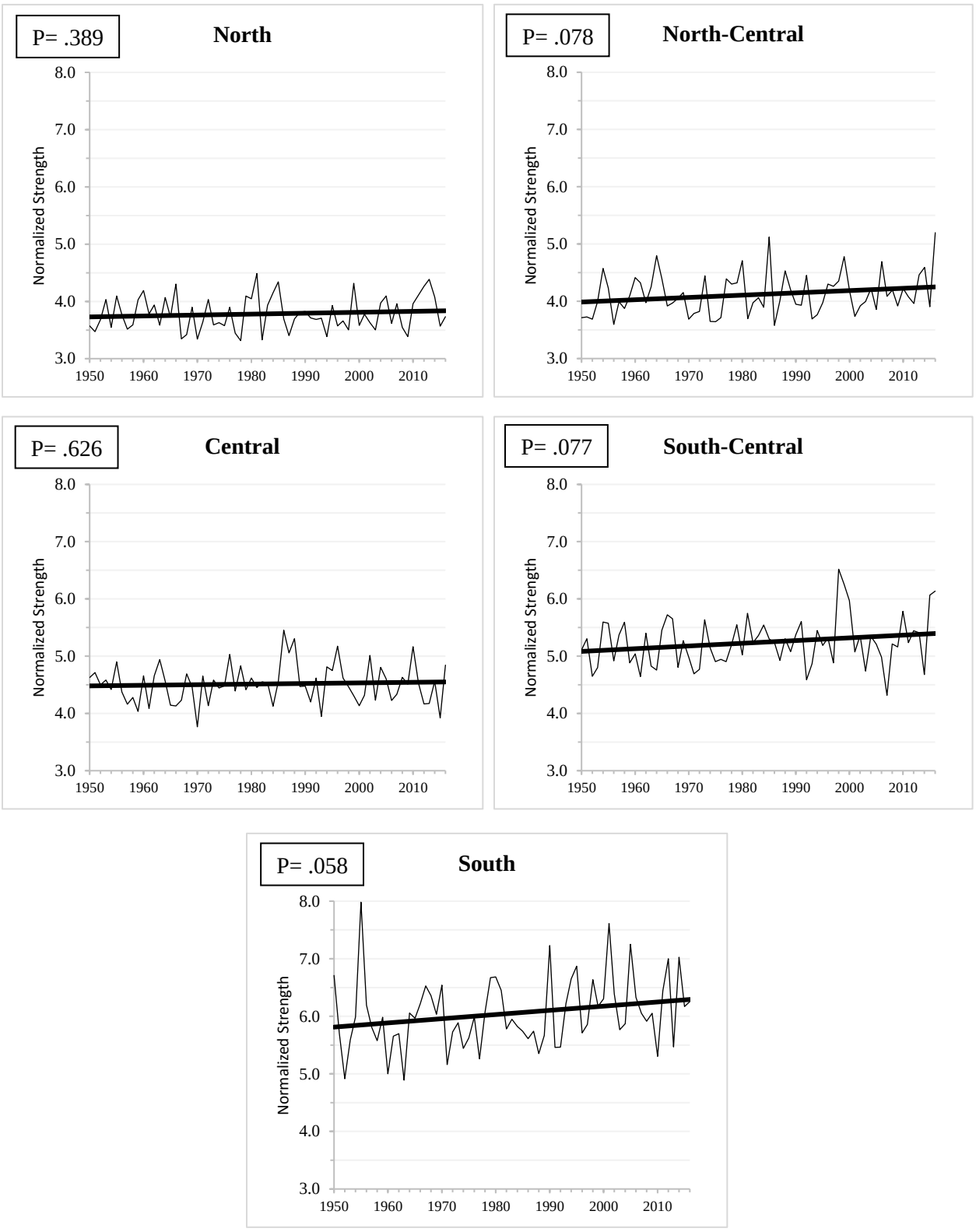

Figure 12: Average Normalized strength of all IPE per year in each latitudinal region

Physiographic (Normalized Strength): Of the five regions, only the Atlantic Coastal Plain ($p = .016$) has exhibited a statistically significant increase in the average strength of events at a 95% CI. This finding is significant however, as the Atlantic Coastal Plain was the only physiographic province that did not exhibit a noticeable increase in the annual recurrence of IPEs. Together, these appear to indicate that while the Atlantic Coastal Plain is not experiencing more IPE per year, the ones that they do experience have become more intense over time. The four other regions display varied results. The Piedmont ($p = .479$) and Appalachian Highlands ($p = .377$) do not display a notable increase in event strength, with the Appalachian Highlands being one of the few regions that has experienced a negative trend in any examined variable. The Ohio-Mississippi Valley ($p = .090$) and Gulf Coastal Plain ($p = .106$) regions have both experienced slight increases in average event strength, a finding which is given increased importance when it is considered that these two regions were the only two regions that have experienced the most statistically significant increase in the total number of annual IPEs. Both coastal plain regions have markedly higher average IPE intensity, which similarly to the two southern latitudinal regions, is due to powerful tropical origin events and ample year-round moisture supply.

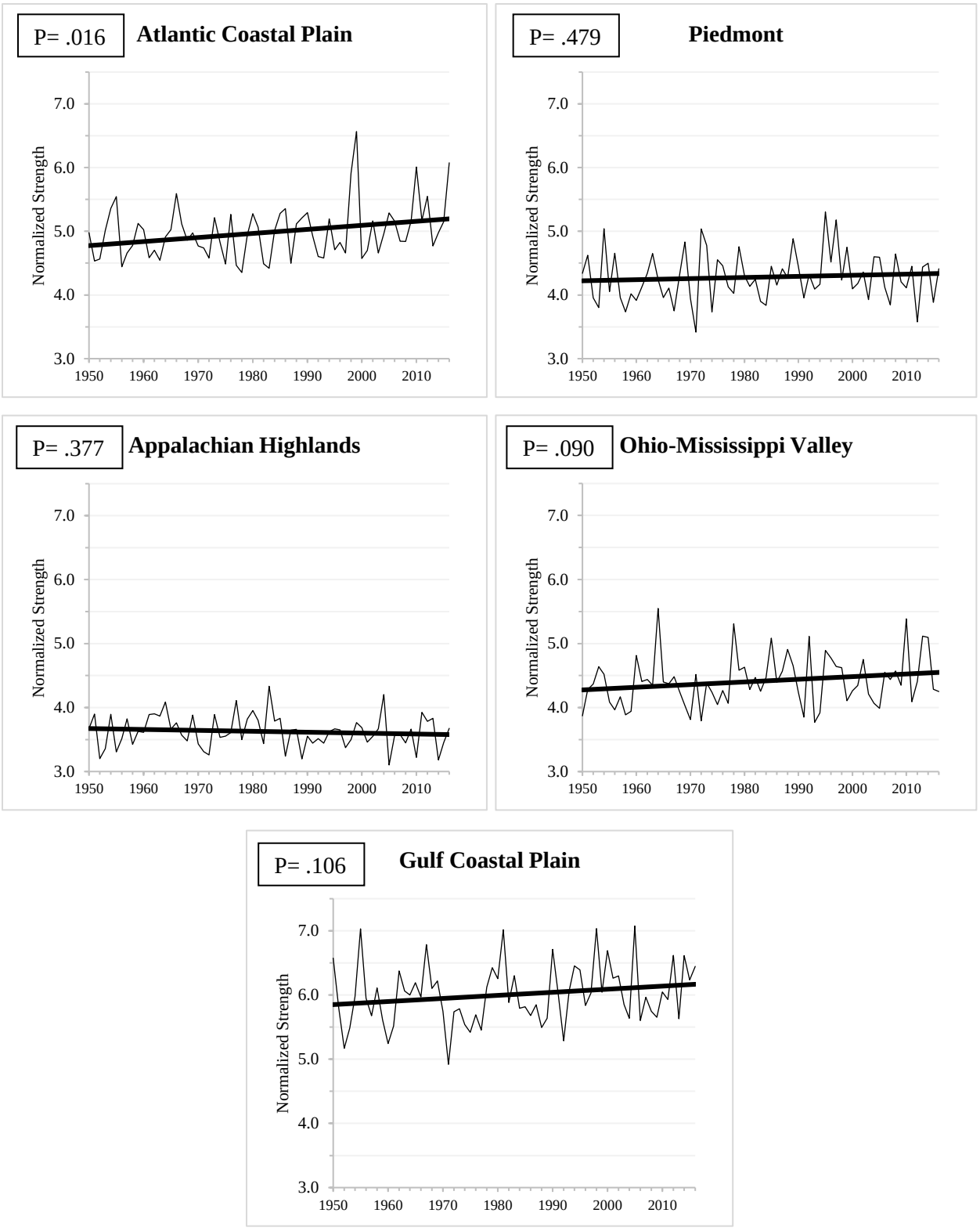

Figure 13: Average Normalized strength of all IPE per year in each physiographic region

Combining the results of the previous sections, it can be stated that IPE have become both more common and stronger across the entire study area since 1950, but the magnitude of these changes has been highly variable across the study area. Physiographically, in the Atlantic Coastal Plain, it was found that IPE have become statistically significantly stronger, but have not become more common. In the Piedmont and Appalachian regions, the average strength of IPE has not increased significantly, but events have become slightly more common over time. In the Ohio-Mississippi Valley and Gulf Coastal Plain regions, IPE have become only slightly stronger over time, but have increased in recurrence at a statistically significant rate. Latitudinally, the northern regions are experiencing a more significant increase in the total number of IPE than the southern regions. Meanwhile, the average strength of events has increased more significantly in the southern regions than in the north, with the northernmost region showing almost no change in this regard. In summary, it can be generally stated that lowland areas outside of the Appalachians have been shown to be more prone to an increase in the strength of IPE, while areas inland from the Atlantic have been shown to be more prone to an increase in the total number of IPE.

Table 1: (Top) 1950 - 2016 IPE trend statistics for the entire study area. (Middle) Latitude and (Bottom) Physiographic sub–region IPE trend statistics. Bold is significant at an alpha level of 0.05. Column titled "increase" shows the increase in the annual total since 1950 based on OLS regression.

Full Study Area Trends	**IPE 1950-2016**		
	p	r^2	Increase
Annual IPE Frequency	**0.013**	**0.092**	**25.502**
Normalized IPE Strength	**0.005**	**0.1166**	**5.87%**
Total Precipitation per IPE	**0.008**	**0.0956**	**0.851 cm**

Latitudinal Region	**Annual IPE Frequency**			**IPE Normalized Magnitude**		
	p	r^2	Increase	p	r^2	% Change
North	**0.049**	**0.0583**	**5.947**	0.389	0.0114	2.8%
North-Central	**0.031**	**0.0696**	**6.574**	0.078	0.047	6.2%
Central	0.079	0.0465	5.452	0.626	0.0037	1.5%
South-Central	0.301	0.0165	2.996	0.077	0.0474	5.8%
South	0.143	0.0327	4.534	0.058	0.054	7.6%

Physiographic Region	**Annual IPE Frequency**			**IPE Normalized Magnitude**		
	p	r^2	Increase	p	r^2	% Change
Atlantic Coastal Plain	0.757	0.0015	1.069	**0.016**	**0.0851**	**8.0%**
Piedmont	0.08	0.0456	3.993	0.479	0.0078	4.3%
Appalachian Highlands	0.066	0.0407	6.131	0.377	0.012	-2.5%
Ohio-Mississippi Valley	**0.011**	**0.0951**	**7.135**	0.09	0.0419	6.1%
Gulf Coastal Plain	**0.028**	**0.072**	**7.187**	0.106	0.0398	5.1%

c. Seasonal analysis

Along with determining whether IPE are becoming more common or stronger over time, this research also seeks to evaluate the seasonality of IPEs. Figure 14 and table 2 show the monthly and seasonal distribution of IPE across the entire study area. This distribution was expected, with distinct peaks during both transitional seasons when unlike airmasses collide more often, and a steady peak in the summer months when there is ample convective energy available. The lone unexpected result in figure 14 is the fact that September experienced the

highest total. This is likely due to a combination of tropical and extratropical inputs, as well as late-summer convection combined with transitional season forcings.

In addition to the utility of knowing the seasonal distribution of IPE through the entire study period, it is also important to know if the seasonality of IPE has changed over time. OLS tests was run on each season to identify whether any individual season is experiencing an increase in the total number of IPE (figure 15; table 2). Every season has experienced a noticeable increase in the total number of IPE per year, with fall having experienced the most significant increase. This increase is also the only one of the four seasons to be statistically significant at a 95% CI ($p = .038$). As such, fall is the only season that was broken down by region, using both latitudinal and physiographic provinces. Regional results can be viewed in table format in table 3.

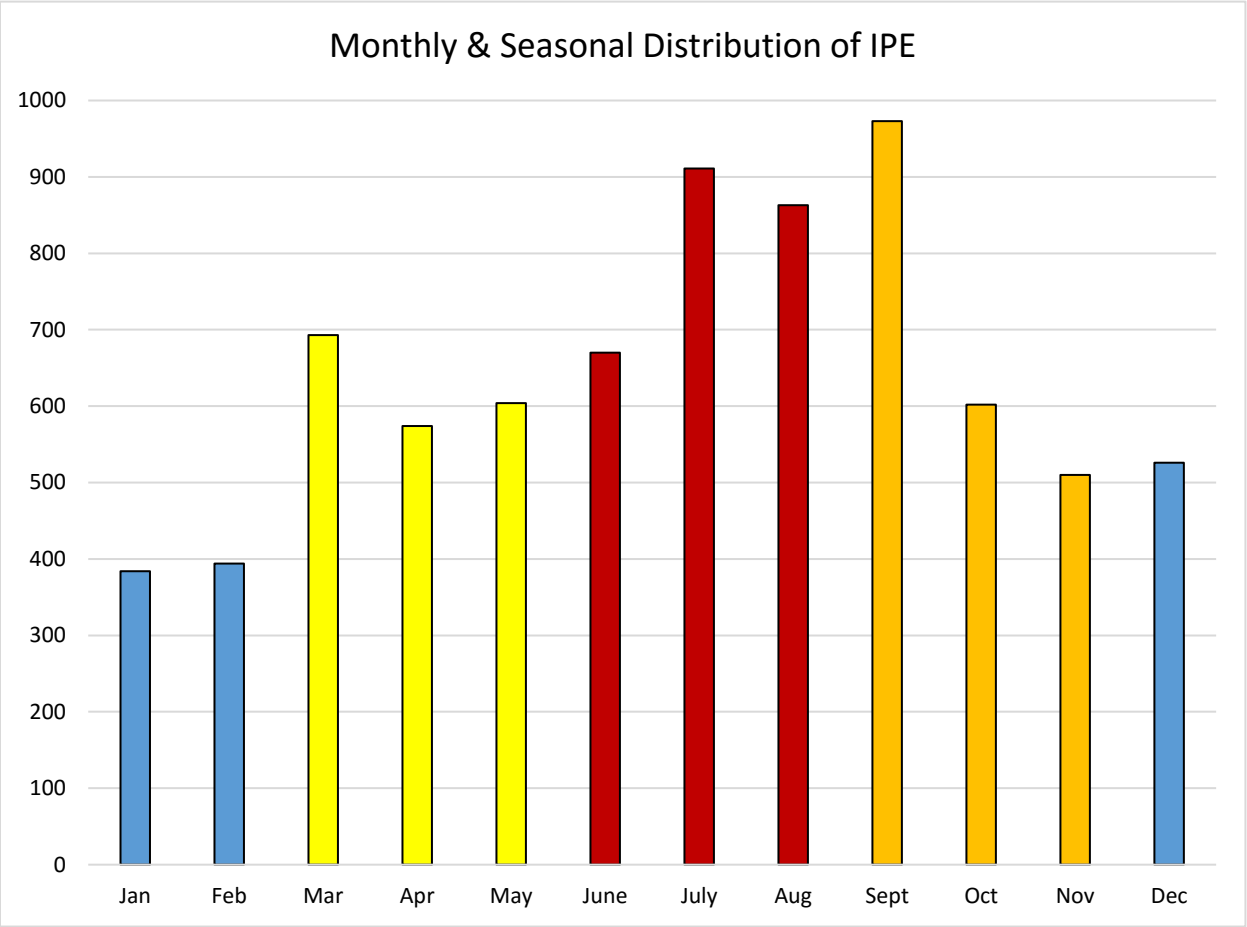

Figure 14: Monthly distribution of all IPE. Colors represent meteorological seasons.

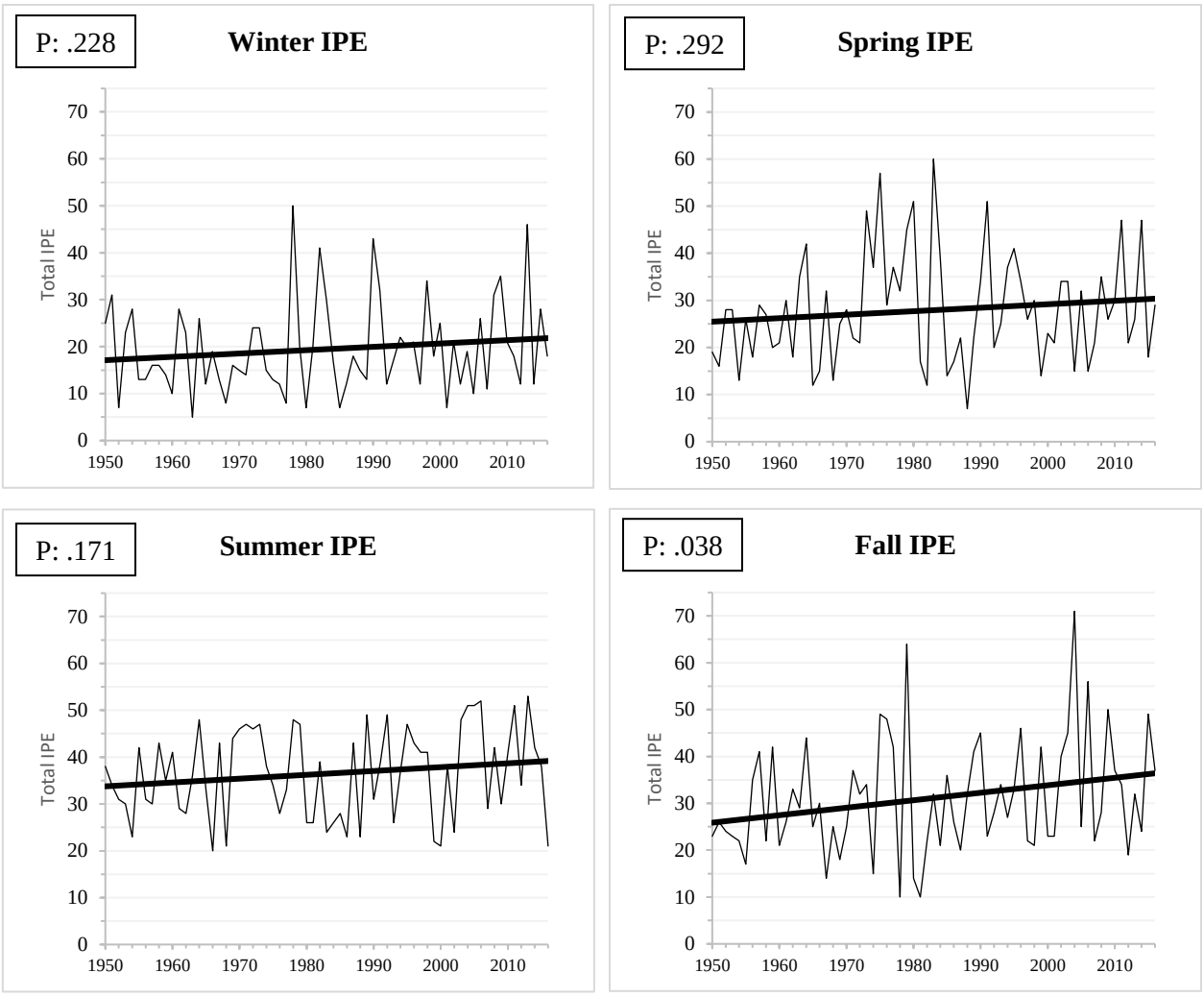

Figure 15: Total number of IPE per year during each season

Table 2: (Top) Monthly IPE distribution. (Bottom) Seasonal IPE trend statistics 1950 - 2016. Bold is significant at an alpha level of 0.05. Column titled "increase" shows the increase in the annual total since 1950 based on OLS regression.

Month	**Monthly IPE Distribution**	
	Total IPE	Percent Contribution
Jan	384	5.0
Feb	394	5.1
Mar	693	9.0
Apr	574	7.5
May	604	7.8
June	670	8.7
July	911	11.8
Aug	863	11.2
Sept	973	12.6
Oct	602	7.8
Nov	510	6.6
Dec	526	6.8
Total	7704	

Season	**IPE 1950 – 2016**		
	p	r^2	Increase
Winter	0.228	0.02	4.686
Spring	0.292	0.02	4.877
Summer	0.171	0.03	5.405
Fall	**0.038**	**0.06**	**10.540**

Latitude (Fall): Of the five latitudinal regions, the North Central (p = .800) is the only one that has not shown a noticeable increase in the total number of Fall IPE. The North (p = .307) region has experienced the most variability throughout the study period, while the Southern (p = .150) region has, on average, experienced the fewest Fall IPE, a surprising result considering the locations proximity to landfalling tropical seasons during the hurricane season. Further research on surface forcing mechanisms associated with these southern fall events would be required to explain this result. The Central (p = .030) and South-Central (p = .008) regions have shown a statistically significant increasing trend in the total number of fall IPE. Both

regions have seen their average annual number of fall IPE increase by approximately 3 events, which is significant given that these 3 events all occur in the span of a three-month period. Remembering that the Central and South-Central regions have 11 and 12 locations within them respectively, an increase of 3 events over such a short amount of time spread across that relatively small number of locations is certainly noteworthy.

Again, further research on the surface forcings associated with these events is required before speculating potential causes, as the South region's small number of annual fall IPE and lack of a significant increasing annual trend potentially rules out an increase in tropical events as being the primary cause. However, the south region has a higher threshold for the total amount of precipitation required for an event to be considered an IPE than the South-Central and Central regions, so an increasing recurrence of high precipitation extratropical events that would be more likely to be classified as IPE in these regions than in the South, remains a likely explanation.

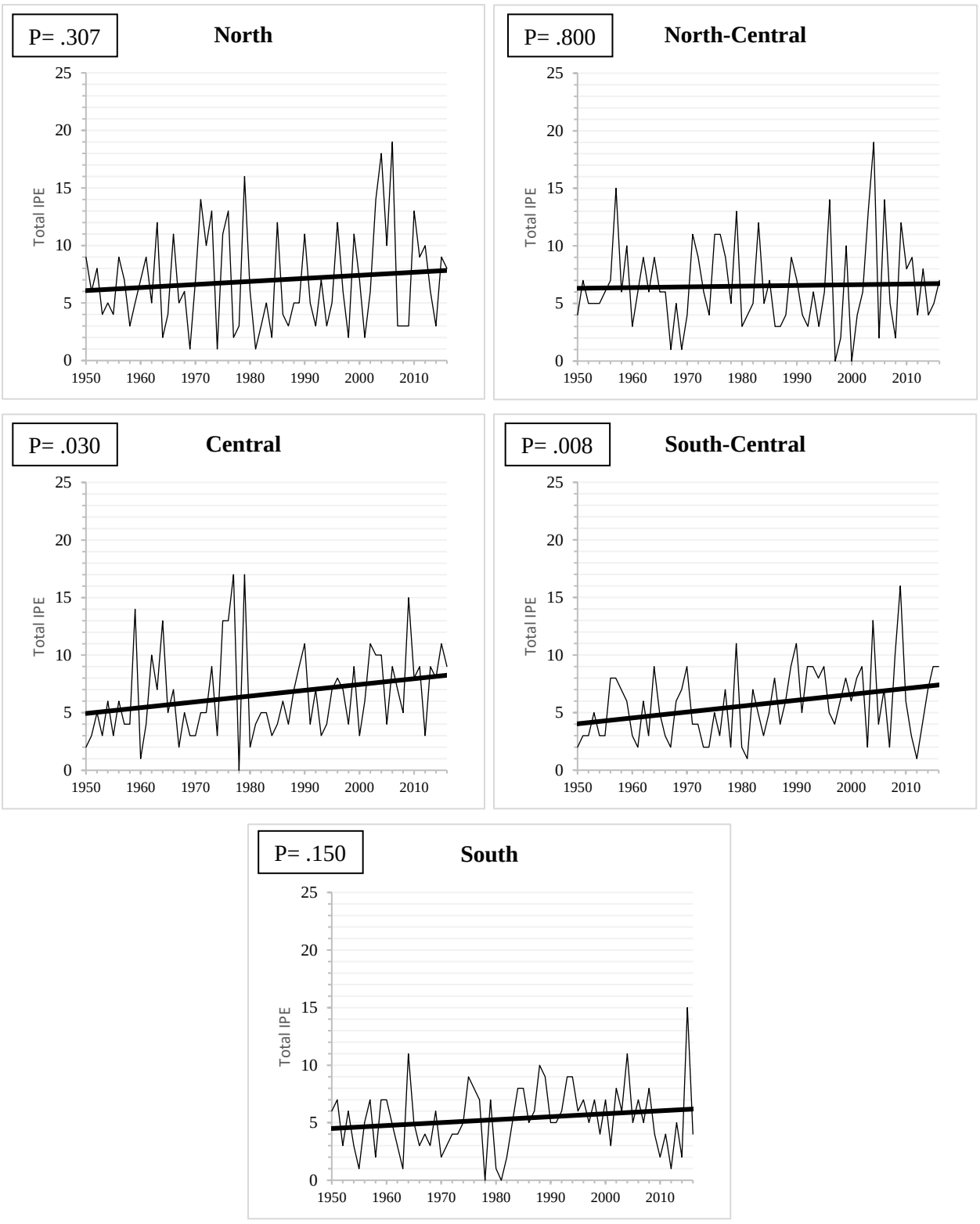

Figure 16: Total number of fall IPE per year in each latitudinal region

Physiographic (Fall): Like the latitudinal division, the physiographic division has only one region that has not shown a noticeable increase in annual fall IPE, the Atlantic Coastal Plain ($p = .777$). This lack of a significant change is driven by large annual variability, which similar to figure 7 on page 24 (which shows the total number of IPE per year across the entire study area), can likely be attributed to its proximity to the Atlantic Ocean and influences from large scale teleconnections that influence synoptic scale trends. These synoptic scale trends have significant influence on the paths of tropical events, and given that peak hurricane season is in the early fall, great annual variability in total fall IPE for this area is to be expected. Despite a lack of a significant increase, the Atlantic Coastal Plain experiences on average the most fall IPE per year, with 2016 being the most active fall to date, with 22 total IPE.

Outside of the Atlantic, the four other regions have experienced at least a modest increasing trend in the total number of Fall IPE, with the Gulf Coastal Plain ($p = .020$) being the lone increase that has been statistically significant. The following section, where the distribution of MT weather types were analyzed, has the potential to reveal if an increase in the recurrence tropical weather types could be a potential explanation for the increase in fall IPE.

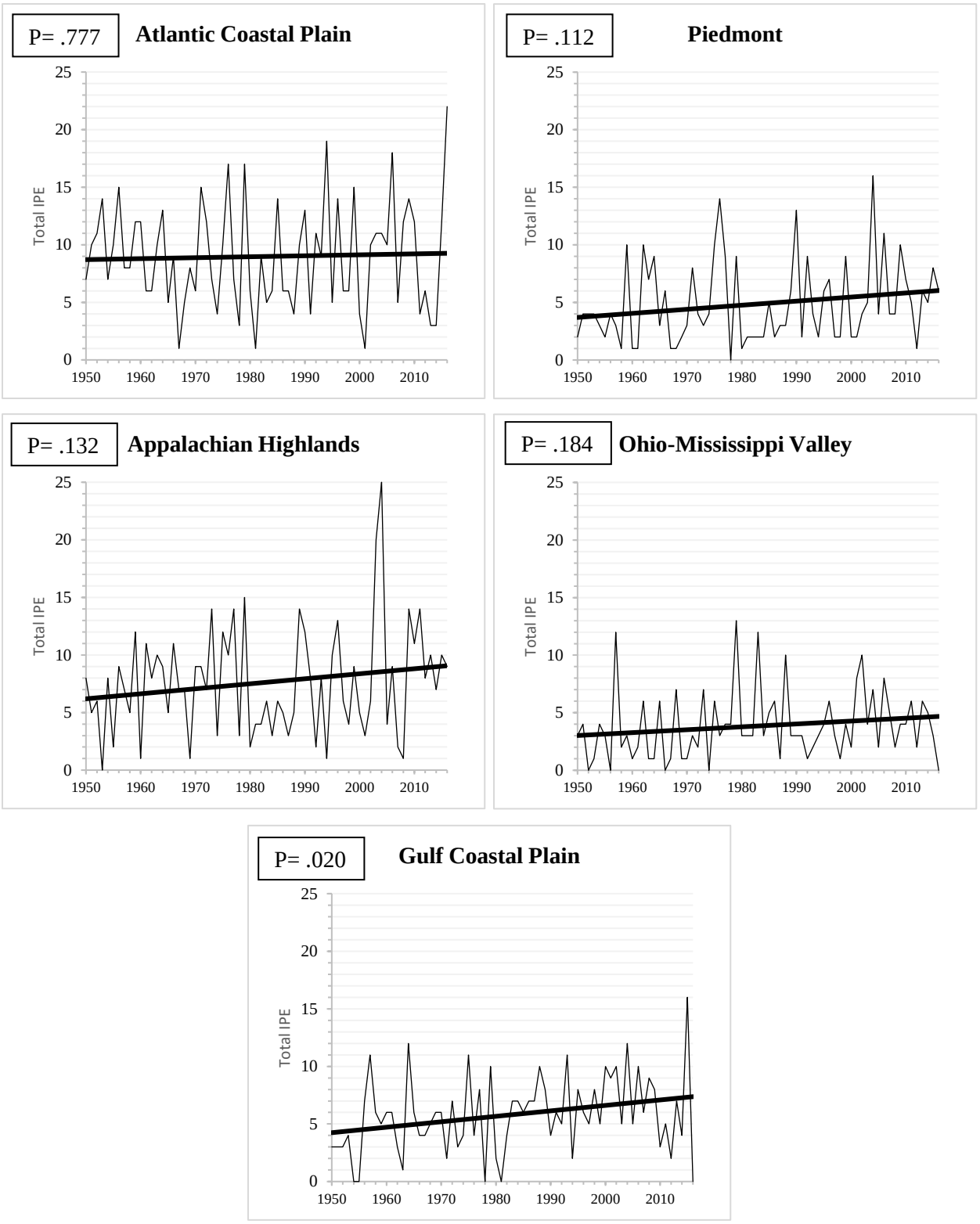

Figure 17: Total number of fall IPE per year in each physiographic region

Table 3: (Top) Latitudinal and (Bottom) physiographic sub-regional trend statistics for fall IPE from 1950-2016. Bold is significant at an alpha level of 0.05. Column titled "increase" shows the increase in the annual total since 1950 based on OLS regression.

Latitudinal Region	**Annual Fall IPE Frequency**		
	p	r^2	Increase
North	0.307	0.015	1.75
North-Central	0.8	0.001	0.41
Central	**0.03**	**0.066**	**3.32**
South-Central	**0.008**	**0.103**	**3.37**
South	0.15	0.03	1.69

Physiographic Region	**Annual Fall IPE Frequency**		
	p	r^2	Increase
Atlantic Coastal Plain	0.777	0.001	0.55
Piedmont	0.112	0.038	2.34
Appalachian Highlands	0.132	0.033	2.87
Ohio-Mississippi Valley	0.184	0.027	1.66
Gulf Coastal Plain	**0.02**	**0.077**	**3.13**

d. SSC Distributions

One of the goals of using the SSC as a classification scheme, in addition to the previously discussed attempt at identifying regionality, was to see if any of the SSC classes are becoming more or less common over time. A change of this kind could indicate changing surface conditions as they relate to extreme precipitation events.

Within the four SSC classes, the most distinct increases have occurred in the Transitional (TR) (p = .078), and Moist Tropical (MT) (P=.000) weather types, with MT holding high statistical significance. MT weather types have increased in average annual recurrence from approximately 17 per year in 1950, to 29 per year in 2016, and the graph of the annual distribution is tightly packed with less variability than many of the previously discussed annual trends. This is a very significant finding, as it indicates that more IPE are occurring as a result of

warm tropical weather types. It is believed that this is due to more common northward and inland encroachment of warm and moist weather types over time, a speculation that was evaluated in the following regional analyses. An increase in northward encroachment of summer time MT weather types was been identified by Senkbeil et al. (2015) in the Eastern US and Canada, but physiographic provinces have not been analyzed for such trends in known previous works.

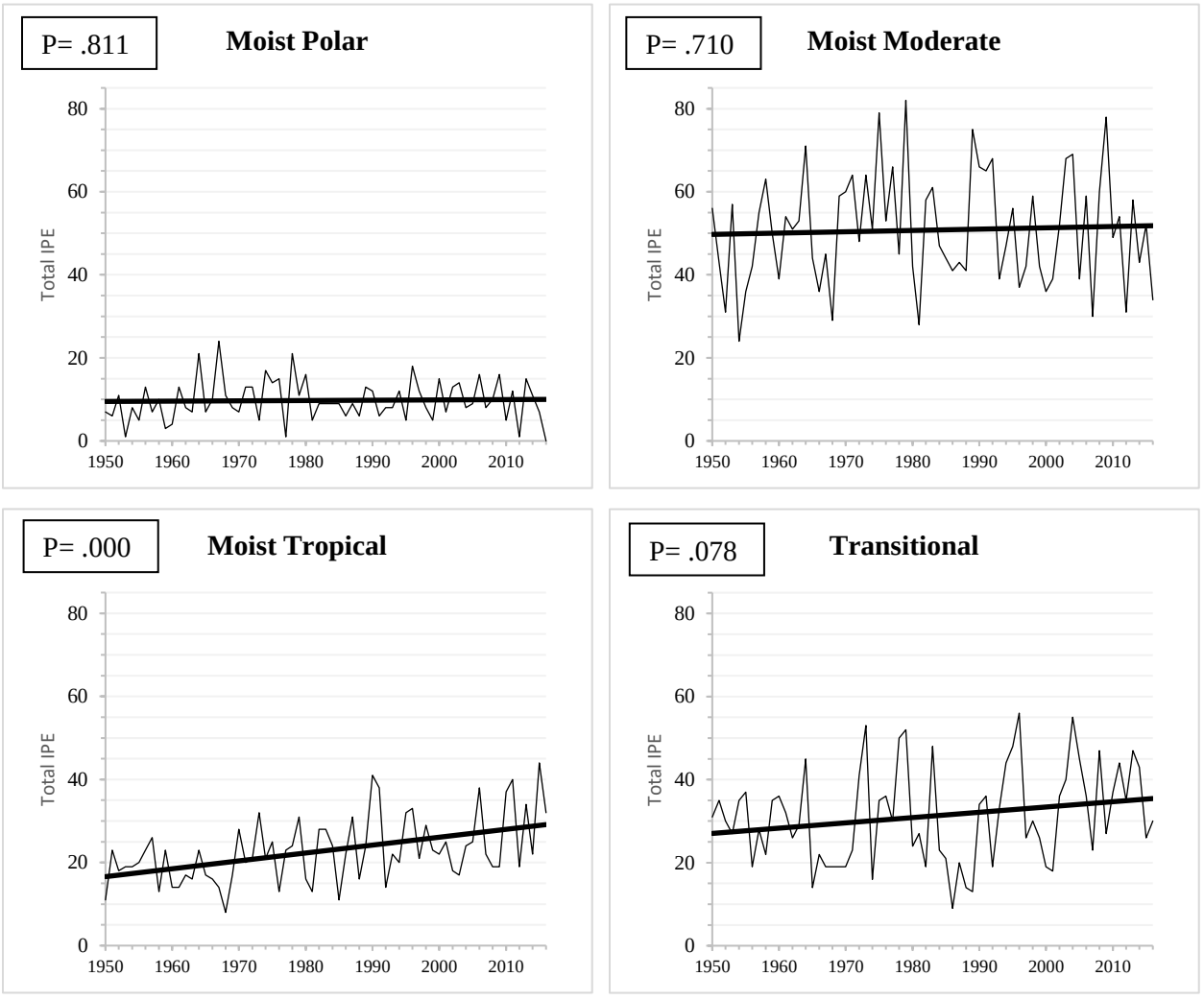

Figure 18: Total number of IPE per year associated with each SSC classification

Latitude (MT): Three regions have exhibited statistically significant increases in the total number of MT weather types at a 95% CI. The only region that has not shown a significant increase is the northern region ($p = .181$), which is not a surprising result due to its distance from the southern source of tropical weather types. The North-Central region ($p = .001$) has experienced the most significant increase in total IPE, while the Central ($p = .008$) and Southern ($p = .011$) regions have also experienced highly significant increases in total IPE. Surprisingly, the South-Central region ($p = .080$) has not experienced a significant change, but this is likely due to an already high recurrence of MT weather types early in the study period. These results appear to confirm the hypothesis that the significant increase in the total number of MT associated IPE per year can be attributed to more common northward encroachment of warm and moist weather types over time. Splitting the study area by physiographic provinces helps to reveal whether, and to what degree, inland encroachment of MT weather types is responsible.

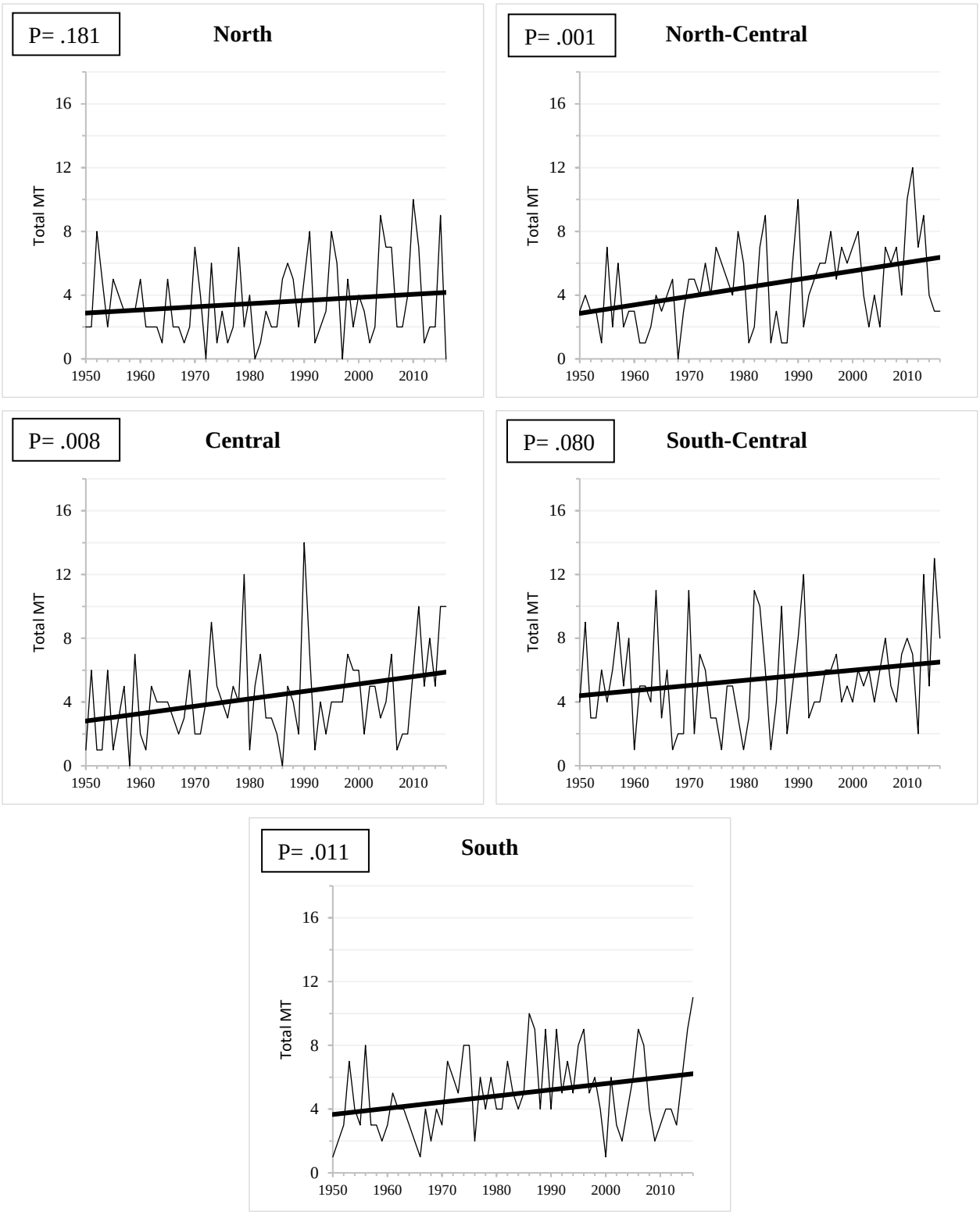

Figure 19: Total number of MT associated IPE per year in each latitudinal region

Physiographic (MT): As with the latitudinal regions, three physiographic regions have displayed a statistically significant increase in the total number of MT associated IPE at a 95% CI. The regions that have not shown a significant increase are the Appalachian Highlands ($p = .102$) which is likely due both to the increasing annual variability since 1980, and the tempering effects of elevation on temperature, and the Atlantic Coastal Plain ($p = .090$) which is most likely due to the inclusion of multiple stations across all latitudinal regions, including the ones that have not shown increasing trends. Both regions have also experienced extreme annual variability since the mid 1970's, making long term trends difficult to identify. The Gulf Coastal Plain ($p = .004$), Piedmont ($p = .000$) and Ohio-Mississippi Valley ($p = .020$) regions have all displayed strongly statistically significant increases in the total number of MT IPE per year. Particularly the increases in the Piedmont and Ohio-Mississippi Valley regions appear to confirm the hypothesis that MT weather types, along with encroaching northward more often, are also encroaching inland more often; however, the lack of significance and increasing annual variability in the Appalachians shows that the increase has not occurred consistently in mountainous areas, largely due to orographic influences on temperature.

Combining both regional results, it can be confidently stated that statistically significant increases in the annual total of MT associated IPE can be largely attributed to more common northward and inland encroachment of the moist and warm weather types that are associated with the MT classification. This finding has the potential to open new avenues for future research utilizing the SSC scheme, particularly to analyze trends in MT weather type recurrence.

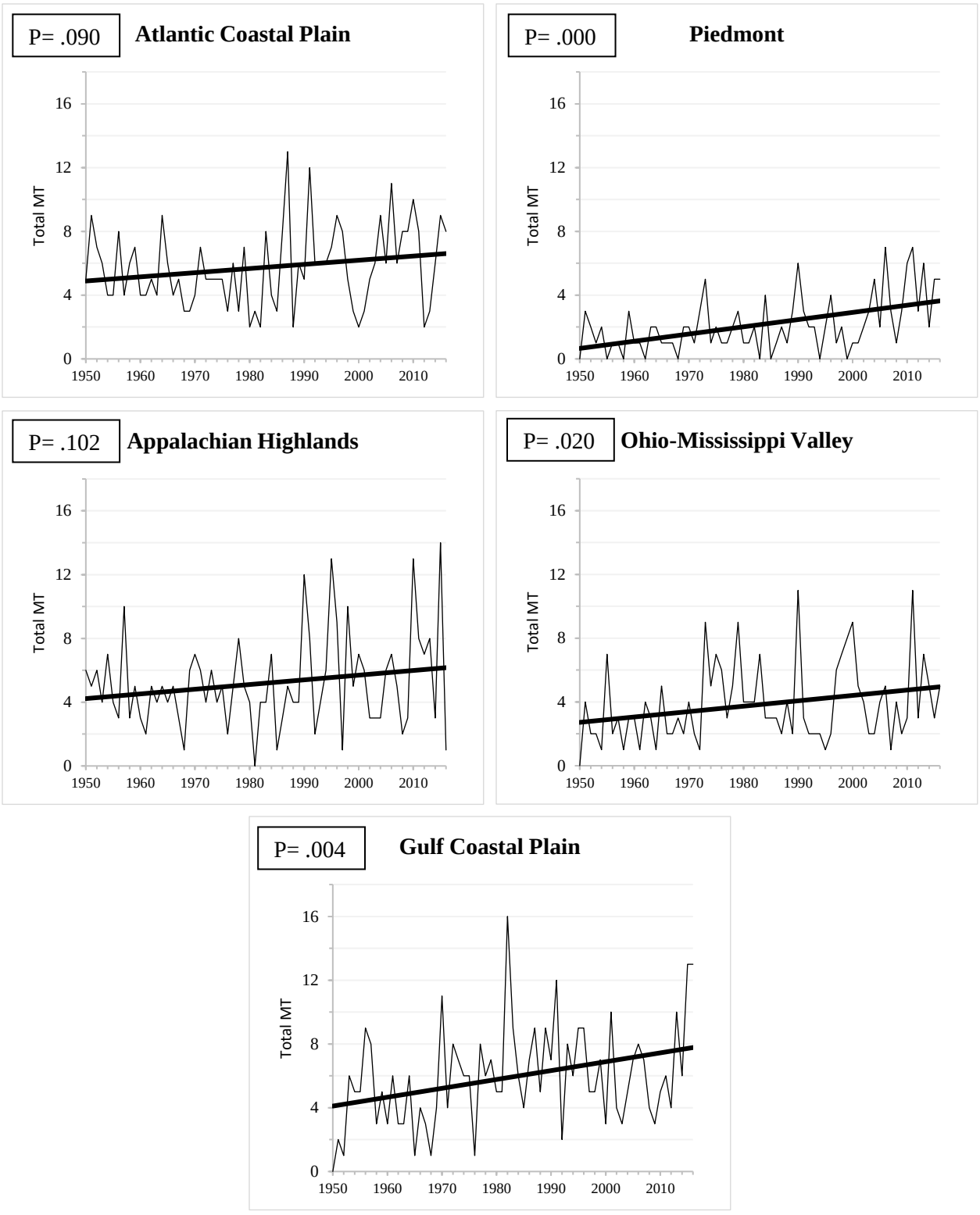

Figure 20: Total number of MT associated IPE per year in each physiographic region

Table 4: (Top) Study area wide SSC trend statistics. (Middle) latitudinal and (bottom) physiographic sub-regional trend statistics for MT associated IPE from 1950-2016. Bold is significant at an alpha level of 0.05. Column titled "increase" shows the increase in number of annual MT IPEs since 1950.

SSC Classification	**IPE Frequency**		
	p	r^2	Increase
Moist Polar (MP)	0.811	0.001	0.49
Moist Moderate (MM)	0.71	0.002	2.10
Moist Tropical (MT)	**0.000**	**0.222**	**12.53**
Transitional (TR)	0.078	0.047	8.40

Latitudinal Region	**MT IPE Frequency**		
	p	r^2	Increase
North	0.181	0.023	1.29
North-Central	**<.01**	**0.161**	**3.51**
Central	**<.01**	**0.101**	**3.07**
South-Central	0.08	0.044	2.11
South	**0.011**	**0.096**	**2.55**

Physiographic Region	**MT IPE Frequency**		
	p	r^2	Increase
Atlantic Coastal Plain	0.09	0.041	1.72
Piedmont	**<.01**	**0.247**	**2.98**
Appalachian Highlands	0.102	0.038	1.94
Ohio-Mississippi Valley	**0.02**	**0.071**	**2.23**
Gulf Coastal Plain	**<.01**	**0.119**	**3.67**

e. Surface Forcings

As was discussed previously, one approach that has been taken for analyzing IPE in previous research has been classifying the surface forcing mechanisms associated with IPE (Keim 1996 & 1997, Powell & Keim 2015). This research seeks only to evaluate the surface forcing mechanisms that are associated with the absolute strongest IPE, and does so from a regional perspective. Using the physiographic regions, each region's top 30 most intense IPE (based on the most intense daily precipitation total of the events, rather than normalized strength)

were identified. Archived surface maps of each of these events were analyzed, and the surface forcing mechanism responsible for the most intense day in each IPE was manually classified. The classification scheme used was similar to that used by Keim (1996), assigning each event to one of the following classifications: airmass, frontal (warm, cold, or stationary), low pressure (concentric, or with frontal influence), tropical (both tropical and extratropical systems), or a combination of these. This phase of the analysis allows for additional synoptic differences between the regions to be identified and discussed.

It is understood that manually classifying events introduces the potential for subjectivity, as not every researcher would classify a given event in the same category, especially if there is not a clear-cut forcing mechanism responsible. This is why the SSC was chosen as the primary classification scheme for this research as a whole, and the surface forcings are evaluated separately. Evaluating surface forcing mechanisms is done to evaluate the triggers for the absolute strongest events in each physiographic region to explore differences between the regions. Additionally, a catch-all category of "combination" was included to help reduce bias for events in which there are two or more surface forcings that are responsible, to prevent a researcher from having to "guess" which forcing they believe is the more dominant of the two. As an example of what would constitute a combination classification, the most common set up for a combination is a stationary front along the coast getting pushed offshore by an advancing cold front. It is hoped that an automated classification scheme can be developed and implemented to explore surface forcings associated with IPEs in the future.

As can be seen in figure 20, the most common surface forcing across the entire region was tropical events, followed by stationary fronts and low-pressure events. This is to be expected, as two of the regions used are coastal areas that are impacted regularly by tropical

events, and inland areas are impacted by precipitation rich extratropical events regularly. The next section examines the surface forcing mechanisms responsible for each physiographic region's strongest IPEs. Distributions of each region's surface forcings can be seen in table 5.

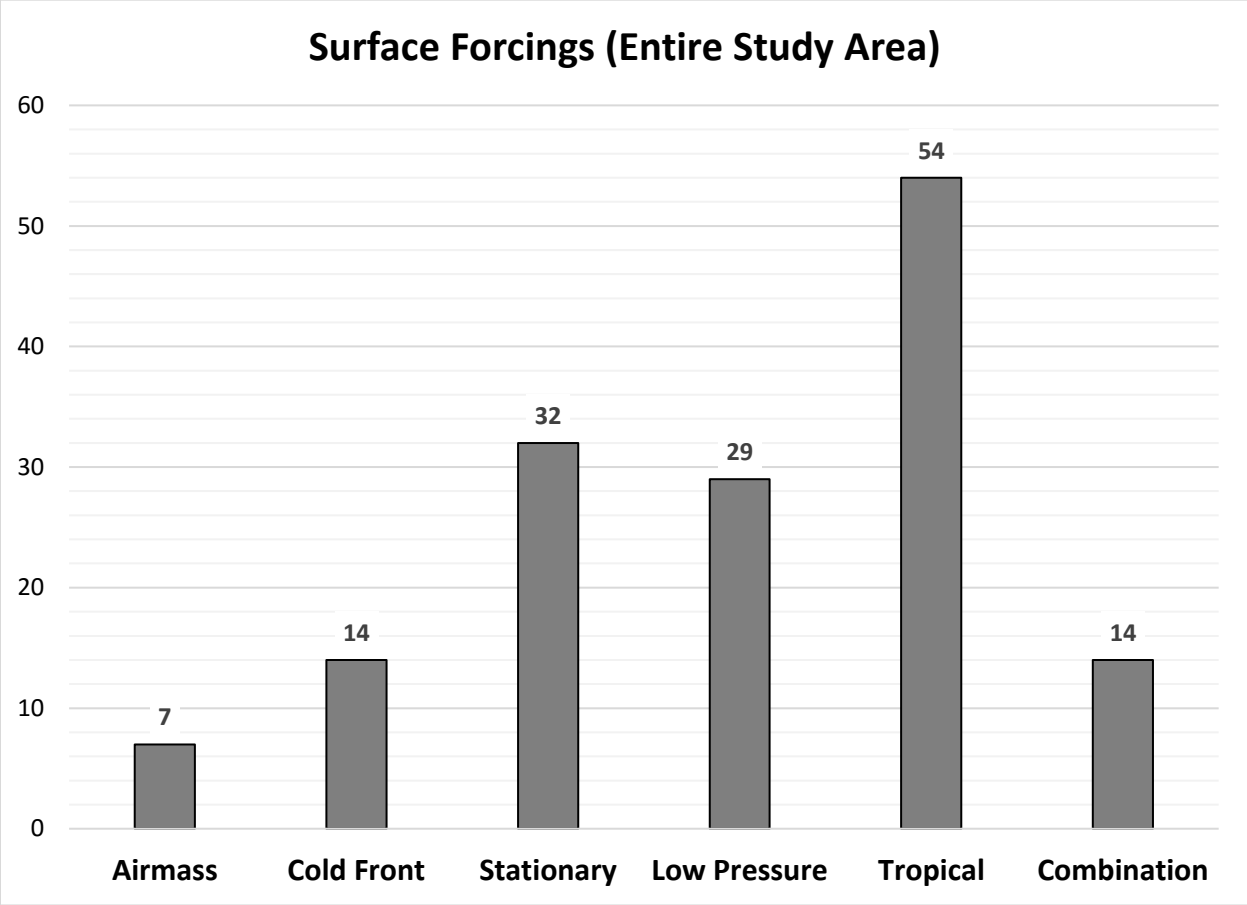

Figure 21: Total number of surface forcing mechanisms responsible for the most intense IPEs based on "top-30" scheme

The Atlantic Coastal Plain closely mimics the distribution of the entire study area, being dominated by tropical events (15), with significant inputs from stationary (7) and low pressure (4) events. This is not surprising, as landfalling tropical systems occur somewhat regularly here,

stationary fronts often park along the southern Atlantic coast, and strong low-pressure systems, either nor'easters or mid-latitude cyclones (MLCs), commonly track through this area.

The Piedmont had the highest recurrence of tropical events, at 17. Keeping in mind that the tropical classification includes extratropical events, this result is not as unexpected as it seems. Most typical events that pass through the Piedmont track generally west to east, and being on the leeside of the Appalachians, orographic inputs often time weaken these types of events (e.g. none of the top-30 events are associated with cold fronts). In the case of tropical events however, they track either south to north, or southeast to northwest. This setup does not allow the Appalachians to weaken the events hydrologically as significantly as they can in other situations.

The Appalachian Highlands had the highest recurrence of low pressure events (10), and had additional significant inputs from tropical (8), and stationary front (7) events. The Appalachians are regularly impacted by MLC type events, as strong MLC's often form just to the west of the study area, and track generally eastward over the region. The Appalachians are also close enough to both the Gulf and Atlantic coasts to receive frequent impacts from extratropical systems.

The Ohio-Mississippi Valley was the lone physiographic province that did not have a particularly significant input from tropical events (3) as it is the most inland, but was rather dominated by stationary fronts (8) and low-pressure systems (7). This region, and the areas just west of it, is a common area of formation for MLC systems, and these events are often spawned as a result of low pressure formation along an existing stationary front, which explains the prevalence these events. This region has experienced the most even distribution of surface forcings, mainly due to a lack of orographic influences, and the absence of oceanic proximity.

Similar to the Atlantic Coastal Plain, The Gulf Coastal Plain mimicked the distribution of the entire study area fairly closely, being dominated by tropical events (11) with meaningful inputs from stationary front events (6). The key difference is that the Gulf CP experienced a higher recurrence of cold front events (5) than any region except for the Ohio-Mississippi Valley, which it is tied with. All five of these events took place between February and April, as winter through early spring is generally the only time of year that the Deep South experiences cold frontal passages. These cold fronts are typically associated with very strong low pressure systems over the Great Lakes region.

In summation, the most intense IPEs in coastal regions and the piedmont are primarily caused by tropical events, and to a lesser degree by stationary fronts and concentric low-pressure events. Meanwhile, the surface forcings responsible for the most intense IPEs in inland physiographic regions are generally more variable, but those regions rely heavily on stationary fronts and concentric low pressures to generate their strongest IPEs. It would be interesting and worthwhile to examine the surface forcing mechanisms responsible for all 99th percentile events in future research if an automated process can be developed, or if the subjectivity of a manual classification technique is somehow reduced to an acceptable level.

Table 5: Surface forcings responsible for each physiographic region's 30 most intense IPE. The most commonly recurring mechanism in each region is bolded.

Physiographic Region	**Surface Forcing Mechanism**					
	Airmass	Cold Front	Stationary	Low Pressure	Tropical	Combination
Atlantic Coastal Plain	1	2	7	4	**15**	1
Piedmont	1	0	4	4	**17**	4
Appalachian Highlands	0	2	7	**10**	8	3
Ohio-Mississippi Valley	4	5	**8**	7	3	3
Gulf Coastal Plain	1	5	6	4	**11**	3
Total	7	14	32	29	54	14

CHAPTER 5

SYNOPTIC ANALYSIS: INTRODUCTION

While chapters 3 and 4 sought to evaluate surface synoptic scale influences, and spatiotemporal trends in IPEs, these final chapters seek to evaluate the upper atmospheric characteristics that are associated with large scale IPEs. While the previous section identified an increase in recurrence and strength of IPEs, and discussed potential and likely causes, an implicit understanding of the upper atmosphere synoptic patterns that create IPEs is essential for accurate modeling and prediction (O'Gorman & Schneider, 2009; Nickl, et al. 2010; Sugiyama, Shiogama, & Emori, 2010; Pathirana, et al. 2014). Variations and trends in mid tropospheric flow have long been used to explain trends in precipitation (Anzelmo & Soule, 1999; Diem, 2006; Gilles, et al. 2011; Pan, et al. 2017), and have also been used to explore other surface parameters, including temperature (Skeeter, 1990; Fall, et al. 2010), and particulate and pollutant variability (Camalier, et al. 2007; Sheridan, et al. 2007) among other variables. The SeUS, a region subject to variable synoptic scale influences on IPE throughout the entire year, such as the seasonal migration of the Bermuda high, or latitudinal location of the jet stream (Schumacher & Johnson, 2006). Understanding the upper level patterns and seasonality that tend to accompany large scale IPEs is given enhanced importance in this region.

While surface level conditions and trends are clearly important to what humans personally experience, specific conditions in mid-tropospheric flow are essential for the development of precipitation. Intense precipitation events only occur under certain rare synoptic situations. Furthermore, large scale intense events that simultaneously impact a large portion of

the study area should only occur under specific, and unusual synoptic patterns. This portion of this research seeks to examine the validity of that claim, and assess whether a set of distinct mid-tropospheric flow patterns can be identified. Previous research has attempted to group or "cluster" sets of commonly recurring circulation patterns over a specific region. Fragoso & Tildes (2007) utilized principal component analysis (PCA) and k-means cluster analysis to classify both rainfall patterns and fundamental large scale atmospheric circulation types associated with intense rainfall events in southern Portugal. Senkbeil (2009) utilized NCEP/NCAR reanalysis data in the Great Plains region to identify commonly recurring flow patterns associated with precipitation in this region. Senkbeil et al. (2011) utilized PCA and cluster analysis to create a classification scheme for extratropical cyclone types, utilizing a manual classification scheme based on storm formation location, as well as reanalysis data. This research utilized various methodologies similar to the two aforementioned studies by Senkbeil and Senkbeil et al., first by attempting to identify commonly recurring 850 & 500mb flow types associated with large scale IPE, and then by utilizing a manual classification scheme based on surface forcings and storm formation location to analyze the mid-tropospheric and surface characteristics of these types of events.

CHAPTER 6

SYNOPTIC ANALYSIS: METHODOLOGY

Large scale IPE were identified by finding days within the study period when eight or more stations out of the 56 used in this research were being impacted by an IPE. Such days were classified as "IPE Days". A total of eight stations was used as the cutoff in order to obtain a large enough sample size to be able to draw meaningful conclusions about commonly recurring trends, while still maintaining a large areal scale. Originally, 10 stations being simultaneously impacted was to be used as the threshold, but this delineation was not able to produce a large enough sample size. Eight stations represents close to 15% of the total number of utilized stations. Typically, all IPE days were exclusive, meaning that large scale IPE only had a single day where eight or more locations were being impacted by an IPE. There were rare situations however where there were multiple consecutive days where eight or more locations were being impacted by IPEs. In these situations, the day with the highest average precipitation totals was used for analysis, as that day could be presumed to be the most synoptically active.

After all IPE days were identified and extracted, NCEP/NCAR reanalysis 850 and 500mb geopotential height values were acquired across the SeUS for each IPE day. This data was acquired on a 2.5 x 2.5 degree grid from 25 – 45° N latitude, 260 - 290° latitude (Figure 22). This grid reaches slightly outside of the bounds of the study area, so that larger regional scale patterns in flow can be evaluated, but is careful not to extend so far as to pick up patterns that do not help explain trends that are experienced in the SeUS.

Once all height values were acquired and organized, they were run through a PCA. Upon completion, all components with eigenvalues greater than 1.0 were saved as variables, and used

as the input for a hierarchical cluster analysis as a means of identifying the optimal number of clusters to retain in an eventual k-means cluster analysis. When the optimal number of clusters to retain was identified, the saved components from the PCA were run through a k-means cluster analysis to identify that number of clusters. Ideally, the k-means procedure separates the dataset into distinct clusters, to identify commonly recurring patterns in mid-tropospheric flow that are associated with large scale IPE. A variety of "seed variables" were included in the PCA in an attempt to create meaningful clusters from the data, by identifying explicit differences in the events that the PCA alone could not identify. These seeds include the primary surface forcing responsible for the event, the month of the year the event occurred, and the average max daily precipitation at each location impacted by the event.

Synoptically meaningful clusters were also manually identified, utilizing methodology similar to that of Senkbeil et al. (2011), based on the surface forcing mechanisms associated with these large-scale IPE, as well as the location of formation of these surface forcings. One of the seed variables mentioned above was the forcing mechanism and formation location of each event. Five broad surface forcing/formation location classifications were identified, and used as the basis for the manual creation of a set of commonly recurring synoptic scale situations associated with large scale IPE. NCEP/NCAR reanalysis data was again be utilized in this situation to create a series of "mean" 500, 850mb, sea level pressure, and 72-hour precipitation maps associated with these five classifications.

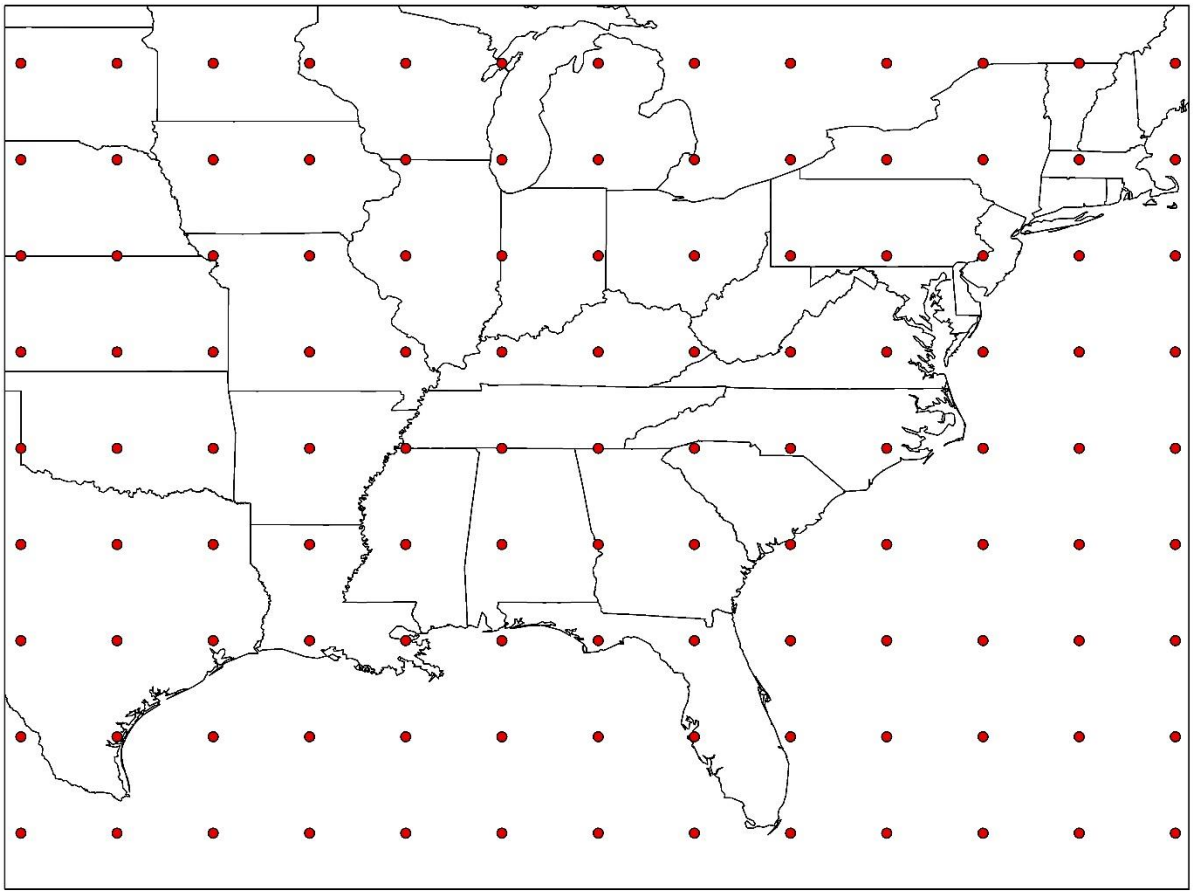

Figure 22: 2.5 x 2.5 degree grid at which geopotential heights and pressure values were taken.

CHAPTER 7

SYNOPTIC ANALYSIS: RESULTS

a. Automated Classification

A total of 133 IPE days for the period from 1950-2016 were identified. Upon collection of all necessary NCEP/NCAR reanalysis data, a PCA was run using only 850 and 500mb geopotential heights without any seed variables. The PCA identified 12 components with eigenvalues over 1.0 that could be used to explain the variance in the dataset (table 4). A total of 52.3% of the variance was explained by the first component, with a gradually sloping decrease in variance after the second component. This distribution and the number of components was substantially different than previous research. In previous research with similar sample sizes, between seven and ten components were typically retained, with two components oftentimes dominating the variance.

Table 6: PCA output using 500 & 850mb geopotential height values for all components with eigenvalues greater than 1.

Total Variance Explained

	Initial Eigenvalues			Extraction Sums of Squared Loadings		
Component	Total	% of Variance	Cumulative %	Total	% of Variance	Cumulative %
1	122.429	52.320	52.320	122.429	52.320	52.320
2	44.846	19.165	71.485	44.846	19.165	71.485
3	16.984	7.258	78.743	16.984	7.258	78.743
4	12.845	5.489	84.232	12.845	5.489	84.232
5	9.247	3.952	88.184	9.247	3.952	88.184
6	8.037	3.434	91.618	8.037	3.434	91.618
7	4.260	1.820	93.438	4.260	1.820	93.438
8	2.246	.960	94.398	2.246	.960	94.398
9	1.979	.846	95.244	1.979	.846	95.244
10	1.658	.709	95.953	1.658	.709	95.953
11	1.593	.681	96.633	1.593	.681	96.633
12	1.341	.573	97.206	1.341	.573	97.206

It was speculated that the most probable cause of these issues was the common recurrence of concentric low-pressure systems, specifically tropical/extratropical events, and MLC's. Since this research is only using a single day's 500 & 850mb geopotential heights for each event, the PCA had difficulty determining whether an event is tropical in origin or an MLC. These are two events that form under drastically different synoptic conditions, but at these two levels of the atmosphere may look quite similar to a process like PCA. In an effort to evaluate that hypothesis, daily surface maps were acquired from the NOAA Central Library, and the surface forcing mechanisms that were primarily responsible for the event were classified. This process confirmed the speculation that a large number of the IPE days were caused by concentric low-pressure events, both tropical and MLC's. Of the 133 IPE days, 98 were associated with either tropical events (45) or some variant of MLCs (53), with the remaining events being caused by frontal events (35). Due to these findings, a methodology similar to Senkbeil et al. (2011),

was used, classifying MLC events into broad categories based on their regions of formation. The surface maps of the MLCs were re-evaluated, and three broad "source regions" were identified for these events. Utilizing these new classifications, the following surface forcing scheme was developed (total number in each class in parentheses):

1. Tropical (45)
2. MLC formed in the Southern Plains (17)
3. MLC formed in the SE, Gulf, or Florida (20)
4. MLC formed in the Midwest, or Northern Plains (16)
5. Frontal (Both cold & Stationary) (35)

These classifications were added to the 850 & 500mb data as a seed variable, coded 1-5, in an attempt to help the PCA identify the distinct differences between the different types of concentric lows. Other seed variables that were added included the month of the year that the event occurred, and the average of each event's "most intense daily total" at each impacted location, to give the PCA an idea of the seasonality and strength of the events. Adding these seed variables did not do enough to show differences that were significant enough to improve the results of the PCA (table 7). Any differences between this iteration and the first one were minute, with only a .5% reduction in the amount of variance explained by the first component, and an additional 13^{th} component added to the existing 12. With these results in mind, it is evident that including these seed variables did not create significant enough changes to warrant further exploration. Future research will seek to identify either additional useful seed variables for this data, or utilize additional variables and methods, along with the utilization of hybrid manual and automated classification schemes.

Table 7: PCA results using seed variables of surface forcing, event strength, and month of the year.

Total Variance Explained

	Initial Eigenvalues			Extraction Sums of Squared Loadings		
Component	Total	% of Variance	Cumulative %	Total	% of Variance	Cumulative %
1	122.803	51.816	51.816	122.803	51.816	51.816
2	45.062	19.014	70.829	45.062	19.014	70.829
3	17.125	7.226	78.055	17.125	7.226	78.055
4	13.037	5.501	83.556	13.037	5.501	83.556
5	9.319	3.932	87.488	9.319	3.932	87.488
6	8.057	3.399	90.887	8.057	3.399	90.887
7	4.328	1.826	92.713	4.328	1.826	92.713
8	2.257	.952	93.666	2.257	.952	93.666
9	2.017	.851	94.517	2.017	.851	94.517
10	1.782	.752	95.269	1.782	.752	95.269
11	1.598	.674	95.943	1.598	.674	95.943
12	1.362	.575	96.518	1.362	.575	96.518
13	1.050	.443	96.961	1.050	.443	96.961

Despite the issues with the original iteration of the PCA, which included only the geopotential height data at 500 & 850mb, the components from that iteration were entered into a hierarchical cluster analysis in SPSS in order to identify roughly how many clusters should be retained. The largest decrease of within group variability occurred between 8 and 7 clusters, suggesting 7 clusters should be retained. The PCA components were then entered into a K-Means cluster analysis, utilizing 7 clusters, as was suggested. The eventual output, at first glance, looked promising. As can be seen in table 8, the K-means cluster did a fair job of separating the 133 days into meaningful clusters, with only two clusters standing out as having low totals.

Table 8: Number of IPE days included in each cluster identified via k-means cluster analysis.

Number of Cases in each Cluster		
Cluster	1	22
	2	18
	3	8
	4	39
	5	29
	6	11
	7	6
Valid		133
Missing		0

These clusters were then analyzed based on their surface maps, and it was found that the separation of clusters was largely ineffective. The k-means did a generally good job of separating events associated with concentric low pressures into different clusters than frontal events. However, many of the clusters were classifying both the various different types of MLC's, and tropical events in the same clusters, which is the exact result the seed variables were aimed to help avoid. A separate k-means test was run which included various combinations of seed variables, to see if they would help prevent this, and results did not notably improve. Another reason for this inability could be that the nature of this research involves the flow characteristics of individual days, while many previous works have involved longer time periods.

b. Manual Classification

While the k-means analysis did a better job splitting the IPE days into clusters, the clusters that were identified are not particularly helpful for the goals of this research. With five distinct classes of surface forcing mechanisms that are commonly associated with large scale IPE

already identified (refer to the list on page 66), this research evaluated the average 500 & 850mb geopotential height values, surface pressure, and precipitation totals that are associated with each of the five distinct surface forcings. This was done by creating daily mean composite maps of geopotential heights at 500mb, 850mb, and the surface of IPE within each of the five surface forcing classifications. These composite maps were created by averaging the observations of a desired variable (in this case geopotential heights and surface pressure values) for each point in the 2.5x2.5 grid of up to 20 different days. The resultant map is an average of all days that are used as inputs. The following section evaluates the key differences and similarities between the 500mb, 850mb, and surface pressure characteristics commonly associated with large scale IPE. For classes with greater than 20 IPE Days (frontal and tropical classes), only the 20 strongest events (based on average highest daily total precipitation) were used. For classifications with less than 20 IPE days, all events in that class were used. Additionally, the average precipitation characteristics of these classes were displayed through a series of "precipitation swath" maps of each classification. This was done similarly to the pressure maps, but utilized average 72-hour precipitation totals at each location for each class. A kriging analysis was conducted for the precipitation totals for each classification to create an interpolated surface of the average precipitation swath associated with each class.

Tropical: This class is responsible for the largest number of IPE days (45). The principal influence that mid-tropospheric patterns have on tropical type events is that they act as a mechanism to either steer events away or towards the coastline. This analysis explores the conditions associated with high precipitation landfalling events. The vast majority of these events occurred during "peak" hurricane season, with 91% of events occurring from August to October, and 49% of events occurring in September. At 500mb, the tropical class is marked by a

deep trough centered over the Mississippi-Alabama border. This trough helps steer these events towards land, most commonly either the eastern Gulf Coast, or the Southern Atlantic Coast. At 850mb, there is a closed upper level low over the eastern Gulf Coast. This closed low corresponds to the most common landfall locations of these events, in a swath from Mississippi to the South Carolina coast. This closed low is present at the surface as well, with sea level pressure (SLP) observations showing the same pattern. These lower level maps combined with the precipitation swath map, indicate that the tropical landfalls that create the most intense large-scale IPE are events that make landfall either (1) near the Florida panhandle and track northward into the Appalachians, or (2) along the coast of the Carolinas, and track north up the coastline, or northwesterly into the Piedmont and Appalachians. Both scenarios can be enhanced orographically, as the events track up the slopes of the Appalachians. In the case of Carolina landfalls, for an east coast tropical system to produce intense rainfall it is critical that tropical moisture is advected into its path during extratropical transition to enhance precipitable moisture (Matyas, 2017). The troughing pattern present over the gulf here is able to provide the necessary moisture for these events.

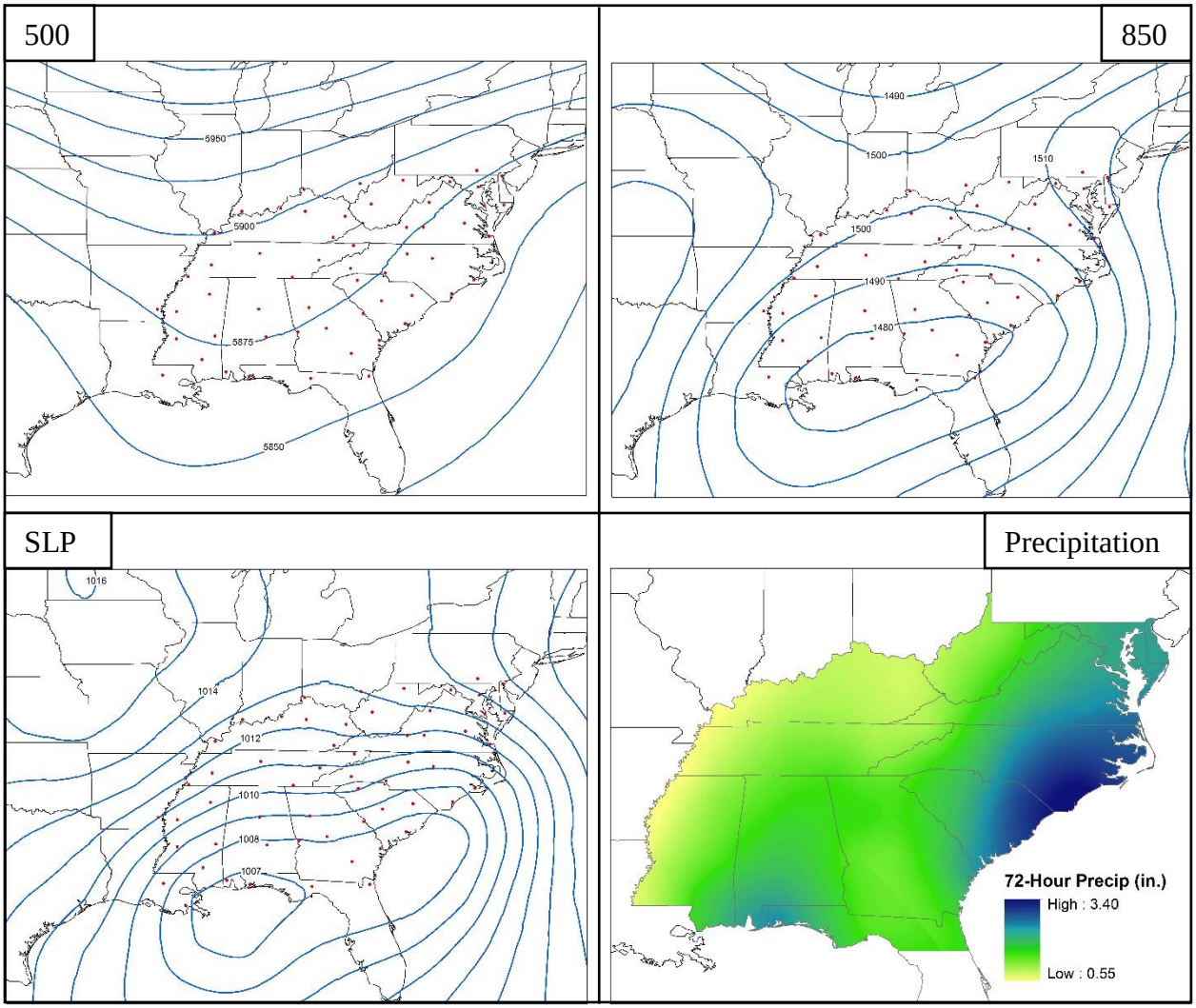

Figure 23: **Tropical** event 500 & 850mb geopotential heights, surface pressure, and 72-hour average precipitation swath.

MLC Southern Plains: This class was named for the often-recurring situation of MLC events forming in the Great Plains region of Texas or Oklahoma, south of 38° N. This class is almost exclusively a winter to spring phenomena, with all but one event taking place between December and May, with the lone exception occurring on November 18th, 2015. Based on seasonal distribution alone, it is clear that these types of events only form during times of the year with turbulent transitional and winter time conditions and significant baroclinicity. At

500mb, these events are marked by a deep trough over the central US, with a ridge just off the Atlantic coast. This pattern leads to events spawned in the Southern Plains tracking through the heart and northern edge of the study area. At 850mb, this pattern is replicated, with a deep trough just along the eastern borders of Nebraska, Kansas, and Texas giving way to Southeasterly flow across the Appalachians. At the surface, a broad low-pressure center is located over Missouri, showing a mean ENE movement towards the Great Lakes with a steep gradient eastward. This class has the lowest mean sea level pressure of any classification examined, which leads to a significant west-to-east pressure gradient. The precipitation swath for these events shows that they often produce their highest precipitation totals in the deep south, principally Alabama and Mississippi with divergence and diffluence promoting uplift. Given that these events most commonly occur during cold or transitional seasons, they advect cold dry air into this moisture rich region, and are able to create IPEs by tapping into the ample moisture and heat provided by the gulf. This moisture then travels inland to the Appalachians, where the events typically weaken before reaching the Mid-Atlantic.

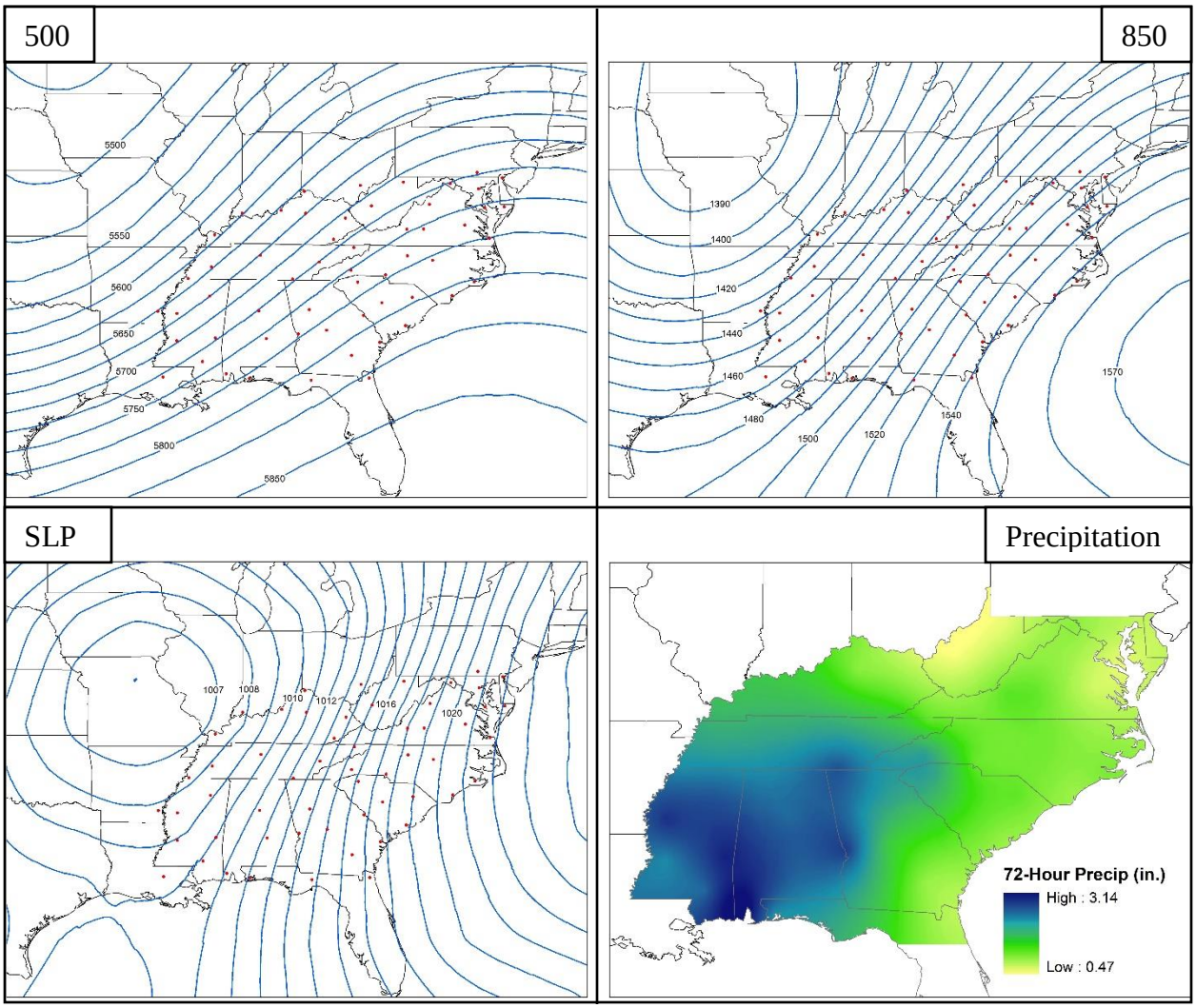

Figure 24: **Southern Plains MLC** event 500 & 850mb geopotential heights, surface pressure, and 72-hour average precipitation swath.

MLC SE, Gulf, or Florida: Another commonly recurring setup for MLC's is formation in the deep south, along the Gulf, or Florida, below 35°N latitude and east of 92°W longitude. This classification has been the most common amongst the three MLC scenarios (20). Similar to Southern Plains events, these events most commonly occurred in winter and spring (60%), however 40% of these events occurred during the fall, making for a fairly even annual distribution outside of summer. At 500mb, this class is marked by a trough over the central US

with a weaker south to north gradient than the other MLC classes. At 850mb, a significant trough is present over the Mississippi River area, with a strong gradient over the gulf that acts to funnel moisture generally northward, and southwesterly flow present east of the Appalachians. At the surface, a central low is located on the Gulf coast, on the border of Mississippi and Alabama. Combined with the southwesterly flow patterns at 500 and 850mb, storms in this class most commonly track northeastwardly from the MS-AL border, through the Appalachians. This is confirmed by the precipitation swath map, which in addition to the hotspot present in the deep south, shows a northeastwardly propagating swath of high precipitation totals along the Appalachians as far north as Virginia. This class is a great visual representation of trough delta cyclogenesis, as the central low presented at the surface is directly in the general region of divergence at the exit (delta) of the trough pattern that is present at both 500 and 850mb.

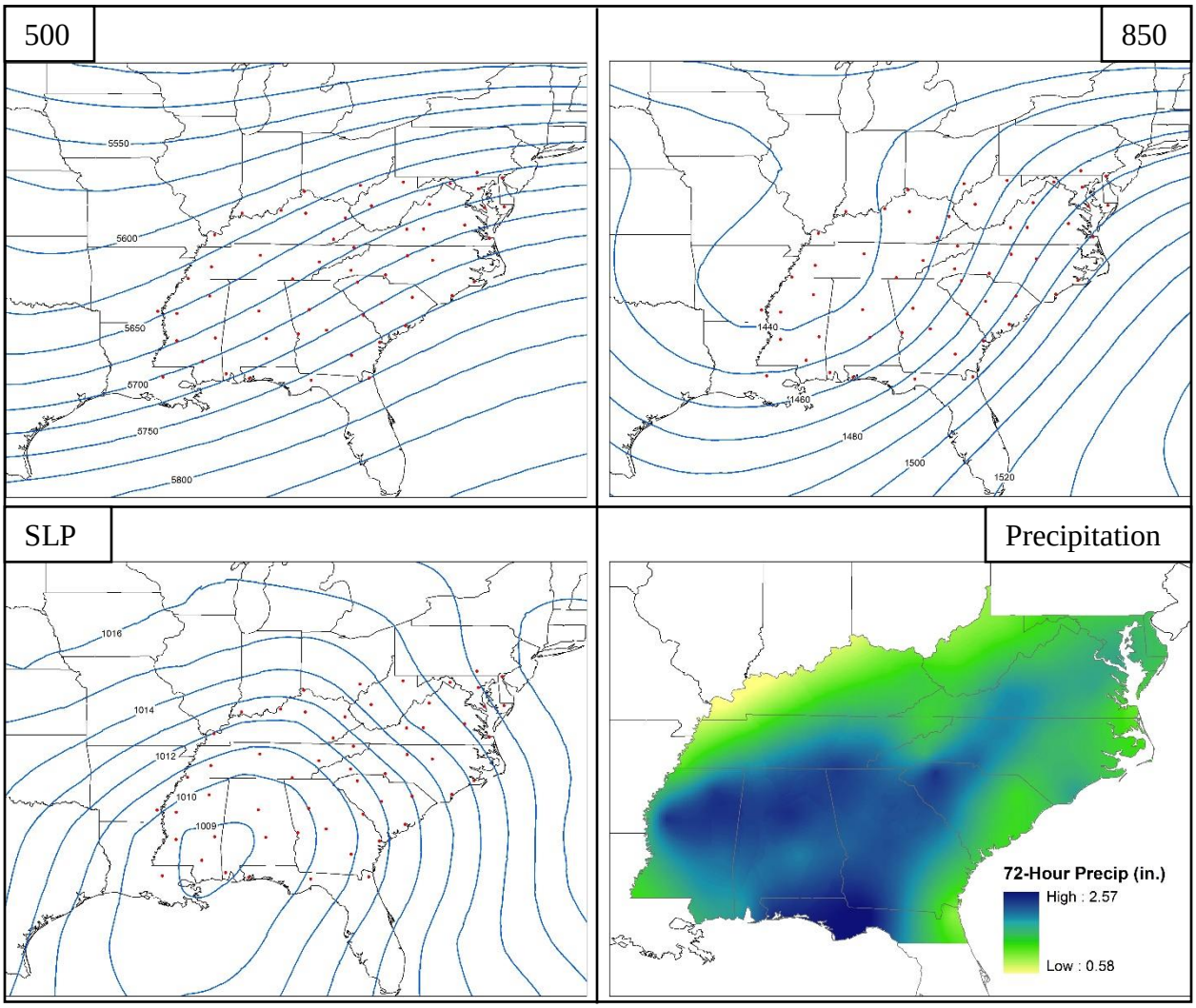

Figure 25: **Southeast, Gulf, and Florida MLC** event 500 & 850mb geopotential heights, surface pressure, and 72-hour average precipitation swath.

MLC Midwest/Northern Plains: A final commonly recurring MLC setup is events that formed in the Midwest or Northern Plains, either north of 38°N, or east of the eastern border of Kansas. The seasonal distribution of the events in this class is fairly even, peaking in the spring (50%), with 25% of events occurring in the winter, and 25% occurring in fall. At 500mb, as with the other MLC classes, this class is marked by a trough across the central US with ridging over the Atlantic coast. This flow pattern is very similar to the pattern displayed by the MLC southern

plains pattern, with the principal difference being that the trough over the central US for this class is not as deep as the trough for MLCs that form in the southern plains, which leads to these events forming farther to the north. The same can be said for the pattern at 850mb, as a trough is present across the central US, but the trough for this class does not cut as deep southward as what is displayed in the Southern Plains class. Additionally, a closed low is present off of the Atlantic coast at 850mb, which helps advect moisture into any events that form under this pattern. At the surface, a nearly closed low is present over Illinois, with a general trough pattern that reaches down to the Louisiana coastline. This is very similar to the pattern displayed by southern plains MLCs, with the key difference being that southern plains events have a stronger central low, that is slightly further to the southwest than this class. This surface pattern, along with the flow pattern at 850mb, helps advect moisture from the Gulf of Mexico northward into the what would otherwise be cool dry airmasses associated with this class. The precipitation swath for this class shows two general hotspots. The first is located over northern Mississippi northward to Kentucky, which is not surprising based on the general east to northeastward track of these events.

The second smaller but intense hotspot is located over the Alabama and Florida Gulf coasts. Archived radar imagery was examined, and it was determined that this area of high precipitation can be explained by warm moist Gulf air being advected northward by the flow patterns present with these events. This moisture is advected in front of a deep southward cutting frontal boundary associated with the central low of the MLC. Mesoscale convective system (MCS) type events oftentimes occur in conjunction with this class, and are able to produce very high precipitation totals in a short amount of time close to the coast as they are amplified by the frontal boundary.

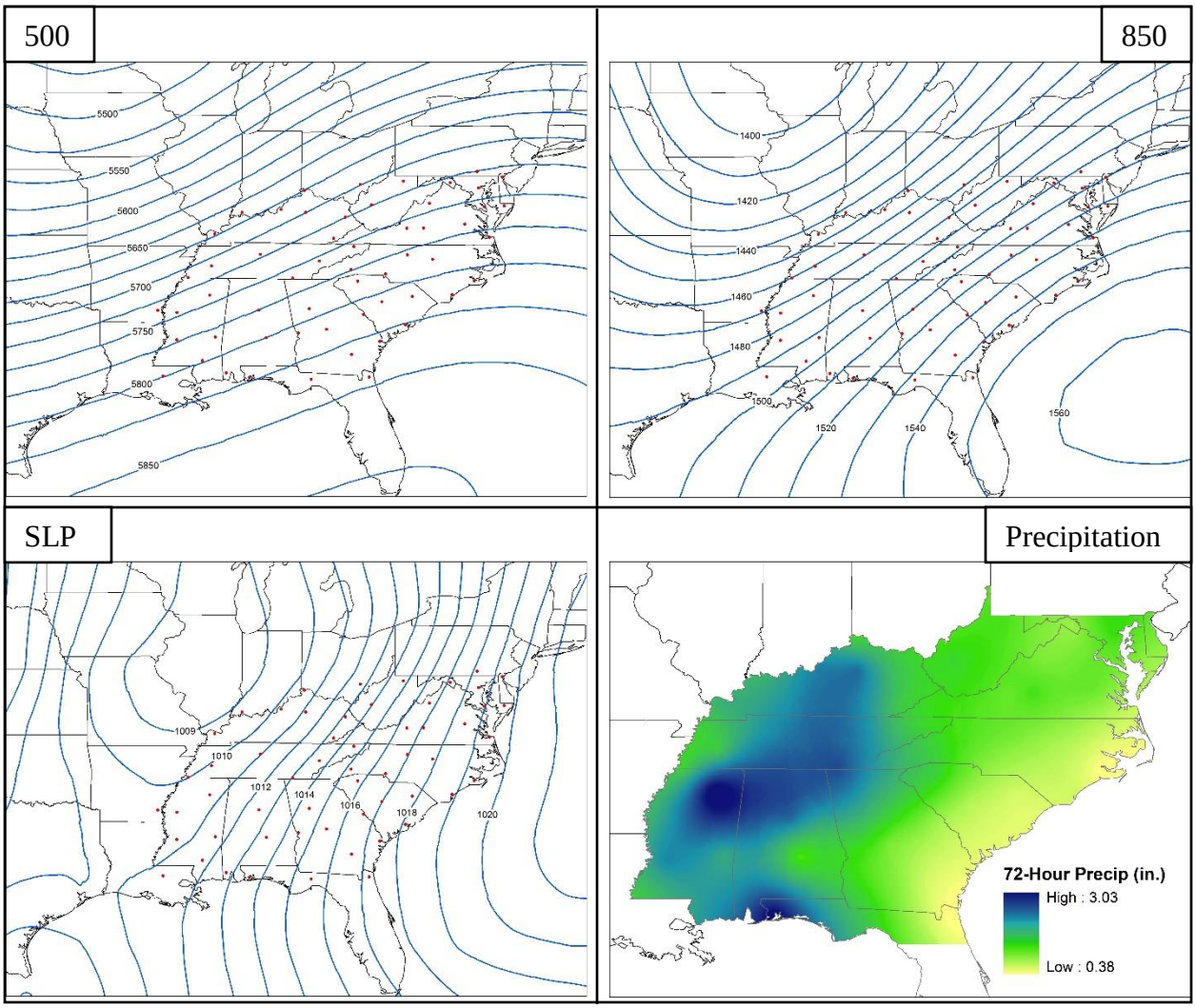

Figure 26: **Midwest and Northern Plains MLC** event 500 & 850mb geopotential heights, surface pressure, and 72-hour average precipitation swath.

Frontal: This class contains both stationary and cold fronts. Trailing only tropical events in recurrence, frontal events (35) are the most evenly distributed classification seasonally, as well as the only classification that contains summertime events (14%). Like all other classes however, this class is dominated by the transitional seasons, with 63% of events occurring in either spring or fall. The trough present in the frontal class is the least intense of all classes, with more zonal flow present at 500mb. At 850mb, a positively tilted trough extends from Wisconsin to northern

Texas, showing the advection of cold northern air into the warm moisture rich southern reaches of this region, which creates the potential for large scale IPEs. The surface map for this class displays a weaker gradient compared to the other classes. Additionally, it shows the location and angle at which frontal events often enter the region, which is complimented by the precipitation swath map showing high precipitation totals over the Ohio-Mississippi Valley. These maps indicate that the most commonly impacted areas within the study region are generally the Ohio-Mississippi Valley and the northern reaches of the Gulf Coastal Plain.

For stationary fronts, the most common scenario that created large scale IPEs was a frontal boundary stalling over the Ohio-Mississippi Valley region, with subsequent cyclogenesis along this boundary leading to large areas of precipitation. Further research will be conducted on the synoptic conditions associated with these types of events, as previous research has proven them to be commonly recurring sources of hydrologically significant events. Any cold front events that were able to produce large scale IPEs were exceptionally slow-moving events. There is a relatively even distribution of stationary fronts (18) versus cold fronts (17).

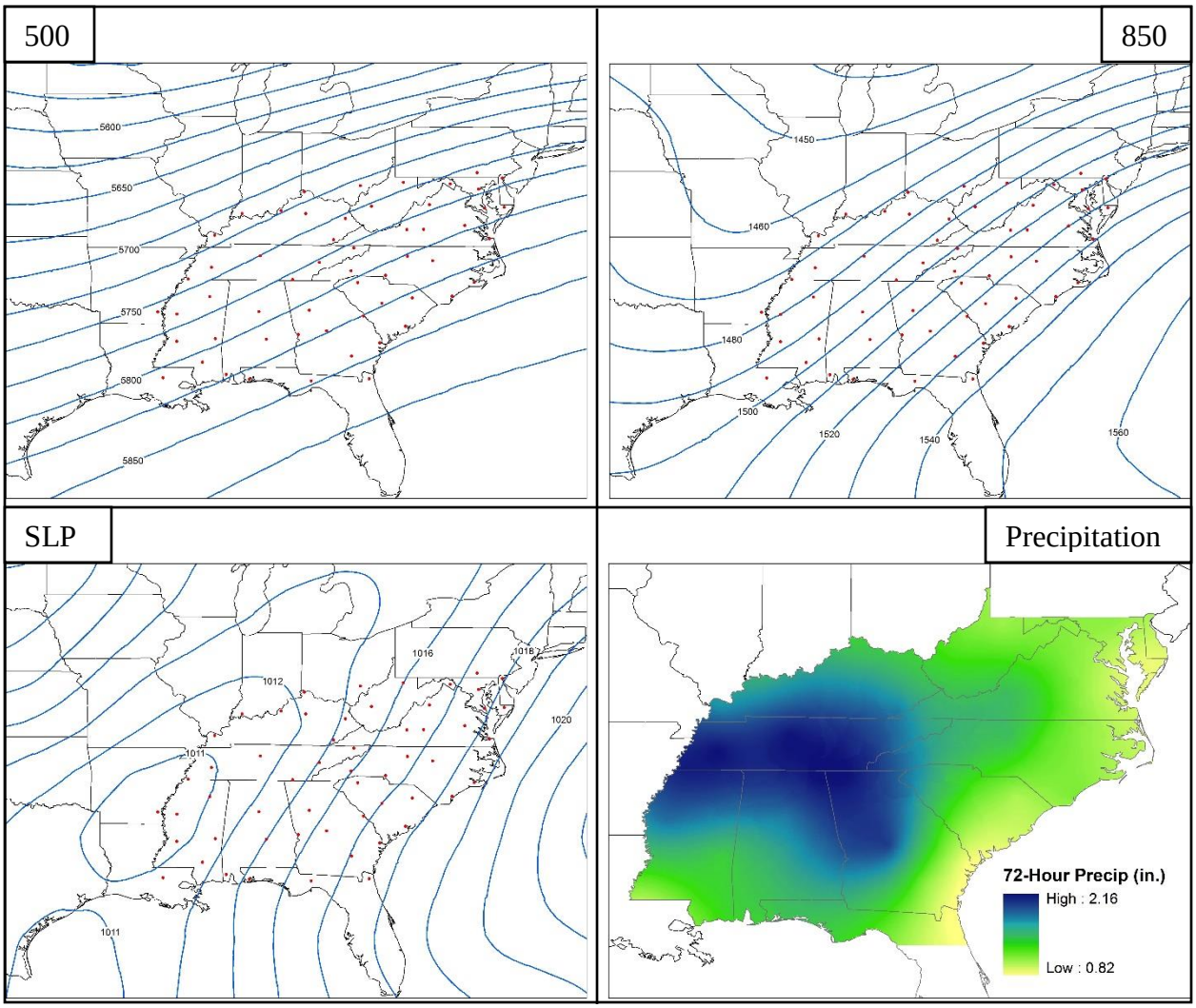

Figure 27: **Frontal** event 500 & 850mb geopotential heights, surface pressure, and 72-hour average precipitation swath.

c. *Statistical Results*

Finally, in addition to visualizing the precipitation trends of these events with the 72-hour swath maps above, the differences in the precipitation characteristics of these events were analyzed to identify whether the differences between them are statistically significant. The data within all five classifications was tested for normality with a Shapiro-Wilk Test, which revealed that the precipitation amounts for two of the five classes (Mid-Western MLC, Southern Plains

MLC) were not normally distributed. As such a Kruskal-Wallis Test (KW), was utilized, and accompanied by Mann-Whitney tests for paired comparisons.

The KW test identified a significant difference between the precipitation totals associated with the five classifications ($p = .03$), which suggests that the classifications used in this manual scheme were distinct, and effectively separated the storm types. As part of the KW output (table 9), each classification was assigned a "mean rank", with larger ranks representing events that produced the most precipitation across the entire study area. In effect, the mean rank value both represents how intense and how localized the events in the classifications are, with larger numbers indicating events that are both intense, and have larger areas of the study area that are impacted by high precipitation totals. The classification with the highest mean rank is Southeastern MLCs, which is supported by the precipitation swath map for these events (Figure 25). There is a large "bullseye" area of high precipitation totals from Mississippi to Georgia, and a tail of high totals that tracks northeastward into the Appalachians. The lowest mean rank was present in the Midwestern MLC class, which is again supported by the precipitation swath map (Figure 26). This classification has a smaller "bullseye" than the other classes, and the entirety of the Atlantic Coast is rarely and lightly impacted by these events. Similar patterns can be

Table 9: Mean ranks of each manual classification, and KW test statistics.

Ranks

	Group	N	Mean Rank
Precip	Frontal	56	132.95
	MLC Midwest	56	118.79
	MLC Southeast	**56**	**165.59**
	MLC Southern Plains	56	135.96
	Tropical	56	149.21
	Total	280	

Test Statistics

	Results
Kruskal-Wallis H	10.715
Degrees of Freedom	4
Significance	**.030**

observed in the other precipitation maps, as the goal of using 72-hour totals rather than single daily totals was to produce a swath that shows general storm tracks.

In conjunction with the KW test, a series of Mann-Whitney (MW) tests were conducted to evaluate the degree of differences of every class against each other. The classes that had the largest differences in their mean ranks, Southeastern MLC, and Midwestern MLC events were the only classes that had significant differences identified. For Midwestern MLCs, the only significant difference was identified between Southeastern MLCs (.001), while the only other notable difference between MW MLCs is Tropical events (.08). For Southeastern MLCs, in addition to the aforementioned significant difference between this class and Midwestern MLCs, a significant difference was also identified between SE MLCs and frontal events (.013), but for no other classes. No significant differences were identified between Southern Plains MLCs and tropical events, which is not unexpected given their modest mean ranks.

Table 10: Mann-Whitney class-to-class significance results, comparing all classes to each other. Bold is significant at an alpha level of 0.05.

Mann-Whitney Significance	Frontal	MLC Midwest/ Northern Plains	MLC Southeast	MLC Southern Plains	Tropical
	p	P	p	p	p
Frontal	_	0.284	**0.013**	0.963	0.278
MLC Northern Plains/MW	0.284	_	**<.01**	0.334	0.080
MLC Southeast	**0.013**	**<.01**	_	0.079	0.524
MLC Southern Plains	0.963	0.334	0.079	_	0.522
Tropical	0.278	0.080	0.524	0.522	_

CHAPTER 8

CONCLUSION & DISCUSSION

This research has yielded a number of significant findings, many of which have created new avenues for future research to be conducted by the author, and others. This research was split into two parts. The first part evaluated surface, synoptic, temporal, and regional trends in IPE. It was found that IPEs have experienced statistically significant increases in both recurrence, and intensity since 1950, and that these trends vary across the different latitudinal and physiographic regions of the SeUS. It can be generally stated that lowland areas outside of the Appalachians have been shown to be more prone to an increase in the strength of IPE, while areas inland from the Atlantic have been shown to be more prone to an increase in the total number of IPEs. Seasonal analysis showed that there has been a statistically significant increase in the number of fall IPEs, with the most significant increase occurring in the southern reaches of the study area.

The SSC was utilized to evaluate surface conditions associated with IPEs. This research is believed to be the first to utilize the SSC for a study of intense precipitation. While moist moderate weather types were the most common classification, IPEs associated with moist tropical weather types have increased at a statistically significant rate. When evaluated regionally, this increase was shown to have been caused largely by more common northward and inland incursion of IPEs associated with this weather type. This phenomenon will be further explored in future research utilizing the SSC.

Finally, a case study was conducted on the surface forcing mechanisms associated with the most intense IPE. It was found that the most intense IPEs in coastal regions and the piedmont are primarily caused by tropical events, and to a lesser degree by stationary fronts and concentric low-pressure events. Meanwhile, the surface forcings responsible for the most intense IPEs in inland physiographic regions are generally more variable, with reliance on stationary fronts and concentric low pressures to generate their strongest IPEs. This case study confirmed a principal finding displayed in previous seed research by the author, that stationary fronts are one of the most commonly recurring surface forcings associated with IPEs. It was initially thought that this would be the case mainly for the Atlantic coast, but this case study revealed that stationary fronts are common creators of IPEs in inland areas as well. The climatology of stationary fronts will be explored in future research.

The second half of this research explored the upper atmospheric and synoptic characteristics associated with large areal scale IPEs. An attempt was made to utilize PCA and cluster analysis to create an automated classification scheme for the 500 & 850mb flow patterns that are commonly associated with large scale IPE. The classification schemes were largely unsuccessful. It is suspected that this was due to the number of concentric low-pressure systems associated with large scale IPEs. This made it difficult for the PCA to identify significant enough differences between the events to separate tropical and MLC events into separate clusters. A variety of seed variables were created to help the PCA identify the inherent differences in these events, but attempts were unsuccessful. This is preliminary research, and additional attempts at an automated classification scheme for flow patterns associated with large scale IPE will be made in future research.

After an automated classification scheme was unsuccessful, a manual classification scheme based on the surface forcing mechanisms was utilized. It was found that all 133 IPE days were associated with either tropical, frontal, or one of three different broad types of MLCs that were classified based on source region. As such, these five commonly recurring forcings were utilized as the five classification groups, and the average 500mb, 850mb, sea level pressure, and 72-hour precipitation patterns were evaluated for each classification. It was found that, unsurprisingly, all classifications were associated with general troughing patterns over the central US, but various differences between the flow patterns of the classes were identified and discussed. Specific influences include how far southward the trough patterns extend on the formation location of the events, the strength of gradients present, as well as locations of closed lows at 850mb and the surface. Precipitation trends were evaluated through a series of 72-hour "precipitation swath" maps, which revealed meaningful information about the areas that are most commonly adversely impacted by these events. Additionally, statistical tests confirmed that each classification's precipitation swaths were statistically distinct, a finding that helps confirm the validity of the manual classification scheme utilized. The classes associated with the highest average precipitation totals were Southeastern MLCs and Tropical events, while Midwestern MLCs produced the lowest precipitation totals.

REFERENCES

Agel, L., Barlow, Qian, Colby, Douglas, & Eichler. (2015). Climatology of Daily Precipitation and Extreme Precipitation Events in the Northeast United States. *Journal of Hydrometeorology*, 2537-2557.

Alexander, L. V. (2006). Global observed changes in daily climate extremes of temperature and precipitation. *Journal of Geophysical Research Atmospheres*, 1-22.

Anderegg, W. R., Kane, J., & Anderegg, L. (2013). Consequences of widespread tree mortality triggered by drought and temperature stress. *Nature Climate Change*, 30-36.

Anzelmo, J., & Soulé, P. (1999). Relationships Between Mid-Tropospheric Flow Patterns and January Precipitation Totals in the Southeastern United States. *Southeastern Geographer*, 75-85.

Barros, A., Hodes, J., & Arulraj, M. (2017). Decadal climate variability and the spatial organization of deep hydrological drought. *Environmental Research Letters*, 1-12.

Berghuijs, W., Aalbers, E., Larsen, J., Trancoso, R., & Woods, R. (2017). Recent changes in extreme floods across multiple continents. *Environmental Research Letters*.

Brody S.D., W.E. Highfield, J.E. Kang (2011). Rising Waters: The Causes and Consequences of Flooding in the United States *Cambridge University Press, Cambridge, UK*

Camalier, L., Cox, W., & Dolwick, P. (2007). The effects of meteorology on ozone in urban areas and their use in assessing ozone trends. *Atmospheric Environment*, 7127–7137.

Collow, A., Bosilovich, M., & Koster, R. (2016). Large-Scale Influences on Summertime Extreme Precipitation in the Northeastern United States. *Journal of Hydrometeorology*, 3045-3061.

Chou, C., Chen, C.-A., Tan, P.-H., & Chan, K. T. (2012). Mechanisms for Global Warming Impacts on Precipitation Frequency and Intensity. *Journal of Climate*, 3291-3306.

Curriero, F. C., Patz, J. A., Rose, J. B., & Lele, S. (2001). The association between extreme precipitation and waterborne disease outbreaks in the United States, 1948-1994. *American Journal of Public Health*, 1194-1199.

Diem, J. (2005). Synoptic-Scale Controls of Summer Precipitation in the Southeastern United States. *AMS Notes and Correspondence*, 613-621.

Emori, S., & Brown, S. J. (2005). Dynamic and thermodynamic changes in mean and extreme precipitation under changed climate. *Geophysical Research Letters*, 1-5.

Fall, S., Diffenbaugh, N., Niyogi, D., Pielke, R., & Ronchon, G. (2010). Temperature and equivalent temperature over the United States (1979–2005). *International Journal of Climatology*, 2045-2054.

Fenneman, N., & Johnson, D. (1946). Physiographic Divisions of the Conterminous U. S. U.S. Geological Survey. Reston, VA: USGS.

Fischer, E. M., & Knutti, R. (2016). Anthropogenic contribution to global occurrence of heavy-precipitation and high-temperature extremes. *Nature Climate Change*, 560-564.

Fragoso, M., & Tildes Gomes, P. (2007). Classification of daily abundant rainfall patterns and associated large-scale atmospheric circulation types in Southern Portugal. *International Journal of Climatology*, 537-544.

Frich, P., Alexander, L. V., Della-Marta, P., Gleason, B., Haylock, M., Tank Klein, A., & Peterson, T. (2002). Observed coherent changes in climatic extremes during the second half of the twentieth century. *Climate Research*, 193-212.

Gilles, R., Wang, S., & Booth, M. (2012). Observational and Synoptic Analyses of the Winter Precipitation Regime Change over Utah. *Journal of Climate*, 4679-4698.

Grose MR, Risbey JS, Whetton PH (2017) Tracking regional temperature projections from the early 1990s in light of variations in regional warming, including "warming holes." Clim Change 140:307–322. doi: 10.1007/s10584-016-1840-9

Heisler-White, J. L., A., K., & Kelly, E. (2008). Increasing precipitation event size increases aboveground net primary productivity in a semi-arid grassland. *Oecologia*, 129-140.

Hurrell, J. W. (1995). Decadal Trends in the North Atlantic Oscillation: Regional Temperatures and Precipitation. *Science (New York, N.Y.)*, 676-679.

IPCC 2013. Climate Change: The Physical Science Basis. Chapter 11: Near Term Climate Change: Projections and Predictability. pages 953 - 1028.

Janssen, E., Wuebbles, K., & Kunkel, K. (2014). Observational and Model based Trends and Projections of Extreme Precipitation over the Contiguous United States. *Earth's Future*, 1-15.

Keim, B. D. (1996). Spatial, Synoptic, and Seasonal Patterns of Heavy Rainfall in the Southeastern United States. *Physical Geography*, 313-328.

Keim, B. D. (1997). Preliminary Analysis of the Temporal Patterns of Heavy Rainfall across the Southeastern United States. *The Professional Geographer*, 94-104.

Knapp, A. K. (2008). Consequences of More Extreme Precipitation Regimes for Terrestrial Ecosystems. *BioScience*, 811.

Krichak, S. O., Breitgand, J., Gualdi, S., & Feldstein, S. (2014). Teleconnection-extreme precipitation relationships over the Mediterranean region. *Theoretical and Applied Climatology*, 679-692.

Kunkel, K. E., Andsager, K., & Easterling, D. (1998). Long-Term Trends in Extreme Precipitation Events over the Conterminous United States and Canada. *Journal of Climate*, 2515-2527.

Kunkel, K. E., Easterling, D., Kristovich, D., Gleason, B., Stoecker, L., & Smith, R. (2012). Meteorological Causes of the Secular Variations in Observed Extreme Precipitation Events for the Conterminous United States. *Journal of Hydrometeorology*, 1131-1141.

Mallakpour, I., & Villarini, G. (2017). Analysis of changes in the magnitude, frequency, and seasonality of heavy precipitation over the contiguous USA. *Theoretical and Applied Climatology*, 345-362.

Matyes, C. J. (2017). Comparing the Spatial Patterns of Rainfall and Atmospheric Moisture among Tropical Cyclones Having a Track Similar to Hurricane Irene (2011). *Atmosphere*.

McGuire, B. (2010). Potential for a hazardous geospheric response to projected future climate changes. *Phil. Trans. R. Soc. A*, 2317-2345.

Meehl GA, Arblaster JM, Chung CTY (2015) Disappearance of the southeast U.S. "warming hole" with the late 1990s transition of the Interdecadal Pacific Oscillation. Geophys Res Lett 42:5564–5570. doi: 10.1002/2015GL064586

Moore, B. J., Mahoney, K., Sukovick, E., Cifelli, R., & Hamill, T. (2015). Climatology and Environmental Characteristics of Extreme Precipitation Events in the Southeastern United States. *Monthly Weather Review*, 718-741.

Nickl, E., Willmott, C., Matsuura, K., & Robeson, S. (2010). Changes in Annual Land-Surface Precipitation Over the Twentieth and Early Twenty-First Century. *Annals of the Association of American Geographers*, 729-739.

O'Gorman, P. a., & Schneider, T. (2009). The physical basis for increases in precipitation extremes in simulations of 21st-century climate change. *Proceedings of the National Academy of Sciences of the United States of America*, 14773-14777.

Pan Z, Liu X, Kumar S, et al (2013) Intermodel variability and mechanism attribution of central and southeastern U.S. anomalous cooling in the twentieth century as simulated by CMIP5 models. J Clim 26:6215–6237. doi: 10.1175/JCLI-D-12-00559.1

Pan, Y., Zeng, N., Mariotti, A., Wang, H., Kumar, A., Sanchez, R., & Jha, B. (2017). Covariability of Central America/Mexico winter precipitation and tropical sea surface temperatures. *Climate Dynamics*.

Pathirana, A., Denekew, H., Veerbeek, W., Zevenbergen, C., & Banda, A. (2014). Impact of urban growth-driven landuse change on microclimate and extreme precipitation - A sensitivity study. *Atmospheric Research*, 59-72.

Powell, E., & Keim, B. (2015). Trends in daily temperature and precipitation extremes for the southeastern United States: 1948-2012. *Journal of Climate*, 1592-1612.

Prein, A. F., Rasmussen, R. M., Ikeda, K., Liu, C., Clark, M. P., & Holland, G. J. (2016). The future intensification of hourly precipitation extremes. *Nature Climate Change*, 1-6.

Prein, Liu, C., Ikeda, K., Trier, S., Rasmussen, R., Holland, G., & Clark, M. (2017). Increased rainfall volume from future convective storms in the US. *Nature Climate Change*, 880-884.

Rogers, J. (2013). The 20th century cooling trend over the southeastern United States. *Climate Dynamics*, 341-352.

Schumacher, R. S., & Johnson, R. H. (2006). Characteristics of US Extreme Rain Events during 1999-2003. *Weather and Forecasting*, 69-85.

Seneviratne, S. I., Corti, T., Davin, E., Hirschi, M., Jaeger, E., Lehner, I., . . . Teuling, A. (2010). Investigating soil moisture-climate interactions in a changing climate: A review. *Earth-Science Reviews*, 125-161.

Senkbeil, J. C. (2009). *The Role of Irrigation on Precipitation in the Great Plains USA.* VDM Verlag.

Senkbeil, J. C., Brommer, D. M., & Comstock, I. J. (2011). Hydrometeorological application of an extratropical cyclone classification scheme in the southern United States. *Theoretical and Applied Climatology*, 27-38.

Senkbeil, J. C., Saunders, M. E., & Taylor, B. (2017). Changes in Summer Weather Type Frequency in Eastern North America. *Annals of the American Association of Geographers*, 1229-1245.

Sheridan, S. (2002). The Redevelopment of a Weather Type Classification Scheme for North America. *International Journal of Climatology*, 51-68.

Sheridan, S., Power, H., & Senkbeil, J. (2007). A further analysis of the spatio-temporal variability in aerosols across North America: Incorporation of lower tropospheric (850-hPa) flow. *International Journal of Climatology*, 1189-1199.

Sheridan, S. (n.d.). *Spatial Synoptic Classification*. Retrieved December 6, 2016, from Kent.edu: http://sheridan.geog.kent.edu/ssc.html

Skeeter, B. (1990). Variations in the Association between Mid-Tropospheric Flow and Surface Temperatures across the United States. *Annals of the Association of American Geographers*, 590-602.

Sugiyama, M., Shiogama, H., & Emori, S. (2010). Precipitation extreme changes exceeding moisture content increases in MIROC and IPCC climate models. *Proceedings of the National Academy of Sciences of the United States of America*, 571-575.

Tootle, G., Piechota, T., & Singh, A. (2005). Coupled oceanic-atmospheric variability and U.S. streamflow. *Water Resources Research*, 1-11.

Trenberth, K. E., Dai, A., Rasmussen, R., & Parsons, D. (2003). The Changing Character of Precipitation. *Bulletin of the American Meteorological Society*, 1205-1217.

Weltzin, J. F., & al, e. (2003). Assessing the Response of Terrestrial Ecosystems to Potential Changes in Precipitation. *BioScience*, 941.

Yang, X., Xie, X., Liu, D., & Wang, L. (2015). Spatial Interpolation of Daily Rainfall Data for Local Climate Impact Assessment over Greater Sydney Region. *Advances in Meteorology*, 1-12.

Zeppel, M. J., Wilks, J. V., & Lewis, J. D. (2014). Impacts of extreme precipitation and seasonal changes in precipitation on plants. *Biogeosciences*, 3083-3093.